

Quantum kernel machine learning with continuous variables

Laura J. Henderson^{1,2}, Rishi Goel¹, and Sally Shrapnel^{1,2}

¹School of Mathematics and Physics, The University of Queensland, QLD 4072, Australia

²ARC Centre for Engineered Quantum Systems, The University of Queensland, QLD, 4072, Australia.

The popular qubit framework has dominated recent work on quantum kernel machine learning, with results characterising expressivity, learnability and generalisation. As yet, there is no comparative framework to understand these concepts for continuous variable (CV) quantum computing platforms. In this paper we represent CV quantum kernels as closed form functions and use this representation to provide several important theoretical insights. We derive a general closed form solution for all CV quantum kernels and show every such kernel can be expressed as the product of Gaussian and algebraic function terms. Furthermore, we present quantification of a quantum-classical separation for all quantum kernels via a hierarchical notion of the “stellar rank” of the quantum kernel feature map. For a particular subclass of CV kernels, we are able to directly extend this notion to the kernels themselves. In all such cases we can quantify the hardness of classical simulability of the quantum kernel. We then prove kernels defined by feature maps of infinite stellar rank, such as GKP-state encodings, can be approximated arbitrarily well by kernels defined by feature maps of finite stellar rank. Finally, we simulate learning with a single-mode displaced Fock state encoding and show that (i) accuracy on our specific task (an annular data set) increases with stellar rank, (ii) for underfit models, accuracy can be improved by increasing a bandwidth hyperparameter, and (iii) for noisy data that is overfit, decreasing the bandwidth will improve generalisation but does so at the cost of effective stellar rank and thus quantum advantage.

Contents

1	Introduction	2
2	Preliminaries	4
2.1	Notation	4
2.2	Introduction to classical kernel machine learning	5
2.3	Background on quantum kernel machine learning	6
3	CV quantum kernels	7
3.1	Representing CV quantum states as holomorphic functions	7
3.2	CV quantum feature maps	9
4	Examples of single-mode CV quantum kernels	10

4.1	Displaced Fock state kernel	10
4.1.1	Closed form & analytic properties	10
4.1.2	Bandwidth tuning	12
4.1.3	Learning experiments	13
4.2	Displacement-phase encoding	17
5	General CV kernels	20
6	Qudit kernels	22
7	Conclusions & future work	23
A	Proof that inner products are positive semi-definite	28
B	Properties of Segal-Bargmann Space	28
B.1	Segal-Bargmann space is a RKHS of the Gaussian kernel	28
B.2	Unitary evolutions of quantum states mapped to holomorphic functions are also holomorphic functions.	30
C	An integration required to calculate the closed form of CV kernels	31
C.1	Explicit calculation	31
C.2	Proof the confluent hypergeometric function $({}_1F_1(b+n; b; \zeta))$ is a product of an exponential and a polynomial	32
D	Properties of the displaced Fock state kernel	33
D.1	Derivation of Eq. (26)	33
D.2	Explicit examples of the displaced Fock state kernel	34
D.3	Showing the displaced Fock state kernel is translation invariant	35
D.4	Showing the displaced Fock state kernel is rotation invariant	36
D.5	Showing the displaced Fock state kernel is a radial kernel	37
D.6	The Fourier transform of the displaced Fock state kernel	37
D.7	Showing the displaced Fock state kernel integrates to π	38
E	Explicit calculation of the general m-mode CV kernel	40
F	Approximating CV kernels of infinite stellar rank	47
G	Calculation of the qudit kernel	50
G.1	Calculation of the qudit kernel from the general multi-mode kernel	51

1 Introduction

The quantum machine learning (QML) community has recently begun to explore whether quantum resources may be useful for kernel machine learning [1–3]. While research has typically focused on improving traditional classical kernel methods, such as support vector machines, classical kernelisation is in fact far more ubiquitous. Kernels, which essentially provide a similarity metric between data points, appear as filters in convolutional neural networks [4], can represent attention matrices in transformer networks [5], are used as training signals for generative networks [6], and can provide a key mechanism for causal discovery [7]. Clearly, there is much to be gained by understanding whether quantum kernels can provide an advantage over their classical counterparts [8–12].

This recent exploration has led to the development of quantum kernel selection tools [13], generalisation bounds [14], optimal solution guarantees [1, 15], and has resulted in several physical implementations [16–19]. The community has learned that although entangled quantum kernels—including those generated by deep parametrised quantum neural networks (PQNN)—are highly expressive, such expressivity typically comes at a cost. This is the so-called “exponential concentration” problem, analogous to the barren plateau problem in quantum neural networks [20]—as quantum kernels become more expressive, they typically also become exponentially harder to learn and less likely to generalise [21–23]. Essentially, the value of the kernel between different datapoints decreases as a function of the size of the problem—for discrete variable quantum kernels, a highly expressive kernel yields exponential concentration. Recent numerical work suggests it may nonetheless be possible to overcome these learning difficulties by manipulating a bandwidth hyperparameter to tune the expressivity of the quantum kernel [24, 25], a technique inspired by bandwidth tuning of classical Gaussian kernels [26]. Finding the sweet spot where the quantum kernel is both learnable and generalises well, but is nonetheless still classically hard to simulate is, however, an open challenge [27]. Robustness to noise also presents a further unexplored challenge to such kernel tuning techniques.

As a consequence, the QML community has to some extent converged on a new quest. Rather than seeking a quantum advantage for kernel machine learning *per se*, physicists are now searching for inductive biases that specific quantum kernels, or families of quantum kernels, may bring to particular ML tasks [22]. The thinking is inspired by the tremendous advantage convolutional neural networks have provided imaging tasks due to their translational invariance [4]. To this end, the group theoretic structure of some specific quantum kernels has been used to exploit structure in certain classical learning problems to prove quantum advantage [16, 17, 28]. As such, there is strong motivation to identify and understand new classes of quantum kernels.

An outstanding key challenge to substantial progress is the theoretically opaque nature of quantum kernels. Classical kernels employ the “kernel trick”—one avoids explicitly evaluating the kernel in feature space by instead using an analytic representation acting in the original data space (e.g. the Gaussian function, or other RBF kernel). This provides direct access to the kernel and permits theoretical analysis. In contrast, quantum kernel values are accessed via estimating inner products through quantum measurement. Thus, quantum measurement expectation values approximate each kernel matrix entry up to some additive error. Functional forms of the kernel are rarely available and theoretical understanding of quantum kernels is somewhat limited.

Interestingly, almost all the work on quantum kernels to date has focused on discrete, finite dimensional quantum systems, such as those generated by parameterised quantum circuits. While a few works have evaluated specific, continuous variable, infinite dimensional quantum encodings [2, 29–32], there is as yet no unifying approach to CV quantum kernels.

In this paper we examine continuous variable quantum kernels through the lens of holomorphic functions. This allows us to present a framework with a very natural taxonomy of kernel “quantumness”, achieved via the notion of the stellar rank of the quantum kernel feature map. Stellar rank ultimately provides useful guarantees as to the hardness of classical simulation [33, 34]. Furthermore, using the holomorphic representation we calculate a closed form expression for an arbitrary CV kernel which allows for insight into the general theoretical structure of CV quantum kernels—every kernel can be expressed as the product of a Gaussian and algebraic function. This structure permits some preliminary intuition into possible trade-offs between bandwidth hyperparameter tuning (to improve

generalisation and learnability) and consequent loss of quantum advantage [27] as kernel values will be close to zero beyond a certain distance.

The paper is organised as follows: in section 2 we introduce relevant mathematical notation and background. In section 3.1 we review holomorphic representations of quantum CV systems (based on [33]). In section 3.2 we formalise how one may define a CV quantum kernel using the tools of holomorphic functions and show it satisfies necessary properties. Section 4 presents two examples of a single-mode encoding, a displaced Fock state encoding and a displacement-phase Fock state encoding. For the displaced Fock state encoding we simulate five learning experiments to verify the expected general behaviour, using a uniform data set and a data set with annular structure. In section 5, we present the multi-mode general CV encoding and show that all finite rank kernels can be expressed as the product of a Gaussian and algebraic function term. We also prove that quantum kernels defined by feature maps of infinite stellar rank, such as GKP and cat-state encodings, can be approximated to arbitrary precision with kernels defined by feature maps of finite stellar rank. General qudit kernels are presented in section 6, where we show that these kernels are a subset of the general multi-mode case. While for particular quantum kernels there are undoubtedly simpler analytic forms, our goal here is to highlight the general form, characterise the stellar rank, and provide insight into some general features that are likely to be applicable to all CV quantum kernels. To this end, we explore the notion of bandwidth tuning and how it affects our example kernels. We conclude with section 7, where we discuss findings and make suggestions for future work.

2 Preliminaries

2.1 Notation

Here we fix notation and formalise the necessary mathematics.

Vectors are denoted in bold unless otherwise specified (e.g. \mathbf{x}) as are matrices, the latter with capital letters only (e.g. \mathbf{X}). Sets and vector spaces are written in mathematical calligraphic font (e.g. \mathcal{X}). Complex numbers will be stated explicitly or as 2-dimensional real vectors, most commonly we use z . Conjugates of complex vectors or matrices are written with superscript asterisk (e.g. \mathbf{x}^*). Overlines instead represent completion of sets, e.g. $\overline{\mathcal{X}}$.

$|\psi\rangle$ will always be a pure quantum state. We reserve n for the Fock state number of such a quantum state. We write all kernels using k , whether they are quantum or classical will be made explicit within the text. We define \mathbb{N}_0 as the set of natural numbers including 0.

Hypergeometric functions are written as ${}_iF_j$, with i, j representing the specific form. Polynomials of x are written as $P(x)$ and Gaussians as $G(x)$. As usual, Γ is the gamma function:

$$\Gamma(z) = \int_0^\infty dt \, t^{z-1} e^{-t} \quad (1)$$

for $\text{Re}(z) > 0$ and $(b)_j$ is the Pochhammer symbol

$$(b)_j := \frac{\Gamma(b+j)}{\Gamma(b)}.$$

The inner product of a specific Hilbert space, \mathcal{H} , is written as $\langle \mathbf{x} | \mathbf{x}' \rangle_{\mathcal{H}}$. Unless otherwise specified, the norm $\|\mathbf{x}\|_{\mathcal{H}}$ is given by $\sqrt{\langle \mathbf{x} | \mathbf{x} \rangle_{\mathcal{H}}}$ where \mathcal{H} is the space in which \mathbf{x} has a well defined inner product.

We define holomorphic functions, denoted by F^* , as complex functions which are complex differentiable in a neighbourhood about every point. F_x^* is a holomorphic function dependent on some classical data $x \in \mathcal{X}$. Stellar functions are a subset of holomorphic functions with finite roots and written as the product of a polynomial and Gaussian term. As n is used as our Fock state number, our stellar rank (the number of complex roots of F^*) is also n .

2.2 Introduction to classical kernel machine learning

The core tenet of kernel machine learning (ML) is the application of linear statistical methods to complex, non-linear data. The data—while not separable in the original data space—can be linearly separated after transformation into a higher dimensional space. The key advantage from kernel methods is the use of the ‘kernel trick’, where one does not need to explicitly compute the data embedding. This trick has found its way into many applications such as ML classification, regression, and clustering [26].

For simplicity, we will describe the supervised learning case to provide the necessary background. We are given some labelled data set, $\{(x_k, y_k), k = 1, \dots, M\}$ and aim to find a mapping $f(x)$ for new unlabeled data points, where $f(x)$ is determined by some structure, pattern or probability distribution within the data. The solution to this learning problem is given by,

$$f^*(x) = \arg \min_{h \in \mathcal{H}} \frac{1}{M} \sum_{i=1}^M \mathcal{L}(h(x_i), y_i) + g(\|h\|), \quad (2)$$

where we define \mathcal{L} as the loss function characterising the performance of the learned function and \mathcal{H} is the Hilbert space of learning functions we are considering [35]. $g(\cdot)$ is a monotonically increasing regularisation function to reduce overfitting, favouring a smooth function with better generalisation.

The crucial step in kernel methods is the encoding of data. Given some data from a space \mathcal{X} we define a data mapping into a Hilbert space \mathcal{H} by a non-linear feature map $\Phi : \mathcal{X} \rightarrow \mathcal{H}$. We usually take the feature map such that the data is not linearly separable in \mathcal{X} but is in \mathcal{H} —commonly achieved by taking \mathcal{H} to be a higher dimension than \mathcal{X} . One such kernel using this mapping is,

$$k(x, x') = |\langle \Phi(x) | \Phi(x') \rangle_{\mathcal{H}}|^2. \quad (3)$$

k uses the inner product in our feature space to form a measure of similarity between data. We consider the kernel to be symmetric (for real valued kernels, taking the absolute value squared is hence unnecessary) and positive semi-definite, i.e., $\forall x_i \in \mathcal{X}$ and any $c_i \in \mathbb{C}^n$

$$\sum_{i,j} c_i c_j^* k(x_i, x_j) \geq 0. \quad (4)$$

Associated to every such feature space is a unique Reproducing Kernel Hilbert Space (RKHS). This is a space of functions that can be constructed as the completion of the span of kernels,

$$\mathcal{H}_{RKHS} = \overline{\text{span}}\{h_{x_i} = k(x_i, \cdot) | x_i \in \mathcal{X}\}, \quad (5)$$

and includes the reproducing kernel, also known as the evaluation functional, h_x , which maps some element of the RKHS h_{x_i} to $h_{x_i}(x) = k(x_i, x)$. The construction of the RKHS permits a solution - by the representer theorem - to equation 2 given by,

$$f^*(\mathbf{x}) = \sum_{\mathbf{x}_i \in \mathcal{X}} c_i k(\mathbf{x}, \mathbf{x}_i), \quad (6)$$

for some $c_i \in \mathbb{R}$ [36].

Formal analysis of classical kernel functions allows one to characterise three key quantities: learnability, expressivity and generalisation. Learnability describes how well the optimal kernel as defined in equation 6 can be found as a function of the size of the problem. Expressivity is used to measure the complexity of problems kernels can linearly classify. If a kernel is universal (i.e. perfectly expressive), it can precisely separate any two given sets from a compact metric space of finite training data [35]. All universal kernels are also characteristic, and can thus be utilised in probabilistic ML applications [37]. In section 4.1 we provide an example of a universal and characteristic CV quantum kernel.

Generalisation theory aims to assess the quality of the learning scheme. Generalisation bounds provide a measure of how well the kernel - given some finite data set from a distribution P - can be applied to randomly sampled data from P that was not in the initial data set. The boundedness of evaluational functions in any RKHS, $\{f \in RKHS : \|f\| \leq B\}$ yields generalisation bounds given by

$$\mathbb{E}_{\mathbf{x} \in \mathcal{D}} |h^*(\mathbf{x}) - f| \leq \frac{2B}{\sqrt{M}}. \quad (7)$$

M is the size of the labelled data set and B is a function of the specific kernel and the loss function from equation 2 [38]. Such approaches are often defined in terms of VC dimension or fat-shattering dimension [39], however, these bounds all represent worst case scenarios and have limited practical relevance. In practice, bandwidth hyperparameter tuning, which essentially changes the length scale of the kernel, is most often used to improve generalisation. If bandwidth is too small, the kernel will treat most new data points as very far from any training observation, while a bandwidth that is too large creates a kernel that will treat each new data point as nearly equidistant to all training observations. Neither will result in good generalization and clearly bandwidth tuning can have a profound impact on learnability and generalisation. Such tuning is similarly computationally very expensive, although recent techniques utilising Jacobian control have shown some improvements [40].

2.3 Background on quantum kernel machine learning

Recently, formal similarities between kernel methods and quantum machine learning (QML) methods have become well established [1]. Essentially, QML methods encode data non-linearly into a higher dimensional Hilbert space in which quantum measurement defines a linear decision boundary. For example, in supervised machine learning we can encode our data in the Hilbert space of the quantum system as $\mathbf{x} \rightarrow |\Phi(\mathbf{x})\rangle$ and then learn the measurement that optimally separates the data. Typically, this state is prepared with some unitary gate operator $U_\theta(\mathbf{x})$ that acts on the vacuum state $|0 \dots 0\rangle$ such that $U_\theta(\mathbf{x})|0 \dots 0\rangle = |\Phi(\mathbf{x})\rangle$. The kernel function is then defined using the Hilbert-Schmidt inner product as,

$$k(\mathbf{x}, \mathbf{x}') = |\langle \Phi(\mathbf{x}) | \Phi(\mathbf{x}') \rangle_{\mathcal{H}}|^2. \quad (8)$$

An important subtlety is that in quantum kernels, we no longer use the same “kernel trick” as in the classical case; kernel entries are not evaluated using a closed form solution applied to the original data space but are rather approximated directly via quantum

measurement. This also means that the RKHS of quantum kernels is rarely characterised, though the existence of the quantum feature map directly implies the existence of a RKHS.

While the majority of quantum kernels are characterised using the qubit circuit formalism, several specific examples of CV quantum kernels exist. Schuld’s excellent summary paper includes a description of a coherent state kernel encoding [2] and Tiwari et. al. construct a mathematical representation of coherent quantum kernels using generalised hypergeometric functions [30]. Ghobadi presents a single-mode squeezed and a single photon (Fock) state quantum kernel and derives a non-classicality witness - a necessary but insufficient condition for quantum advantage - for each [29], and Bowie et. al. describe an experimental platform which exploits Hong–Ou–Mandel interference to evaluate a kernel based on a temporal encoding [32]. There is to date, however, no unifying framework from which to understand these individual results. In the following section we introduce the relevant background on holomorphic representations of CV quantum states to understand our approach.

3 CV quantum kernels

3.1 Representing CV quantum states as holomorphic functions

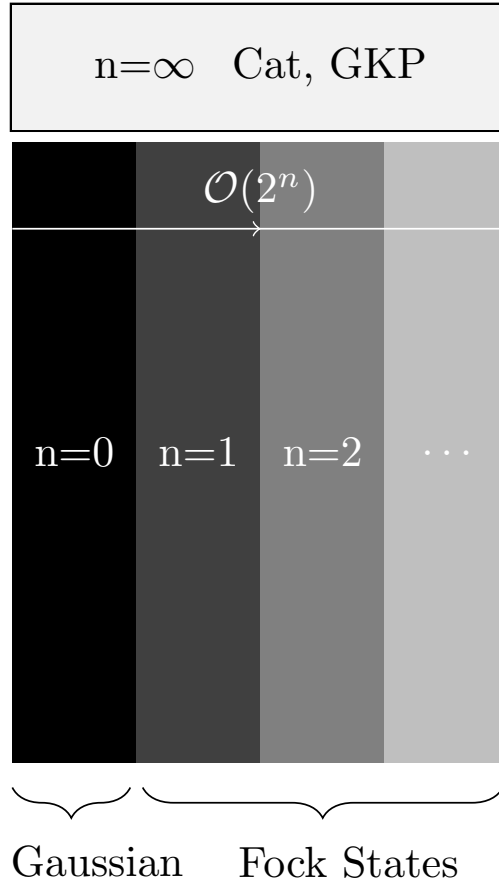


Figure 1: Adapted from [33]. The taxonomy of stellar functions representing CV quantum states. The $n = 0$ states are classically simulable and include, but are not limited to, coherent states, thermal states, and (multimode) squeezed states. As the stellar rank, n , increases, the strong simulability of the state increases exponentially. The $n = \infty$ states are not part of the stellar hierarchy, but can be approximated arbitrarily well by states of finite stellar rank.

Quantum information processing (QIP) is often separated into two paradigms: discrete variable QIP and continuous variable QIP. The former utilises finite dimensional Hilbert spaces and qubits or qudits, whereas the latter utilises infinite dimensional Hilbert spaces and qumodes. In the discrete case, non-Clifford operations or magic states are identified as necessary for bounded error quantum polynomial (BQP) complete, non-classically simulable, computation [41]. Analogously, non-Gaussian operations or non-Gaussian states are identified as necessary for BQP-complete computation in the CV setting [42]. In recent work, Chabaud et. al. present a measure of non-Gaussianity which permits a more nuanced quantification of the computational power of CV quantum computing platforms [33]. In this approach, CV states are fully characterised by holomorphic functions. Such functions can be thought of as quasi-probability distributions, similar to Wigner functions or Husimi functions. In the CV case, we can decompose a finite rank holomorphic function as a stellar function - a product of a Gaussian and polynomial in z . The polynomial is characterised by its roots and accounts for the non-Gaussianity of the quantum system [33].

For single bosonic modes, with orthonormal basis $\{|n\rangle\}_{n \in \mathbb{N}_0}$, we can encode our state using the canonical coherent states as,

$$|z\rangle_\infty = \sum_{n \geq 0} \frac{z^n}{\sqrt{n!}} |n\rangle. \quad (9)$$

One can treat these as phase-space wave functions of a corresponding quantum state. Instead of representing quantum states as infinite countable vectors as seen in the Fock state description, they can be characterized as holomorphic functions through the transformation,

$$|n\rangle \leftrightarrow \left(z \mapsto \frac{z^n}{\sqrt{n!}} \right), \quad (10)$$

for all $n \in \mathbb{N}_0$. Hence a particular quantum state, decomposed into its Fock basis as $|\psi\rangle = \sum_{n \geq 0} \psi^{(n)} |n\rangle$ can be transformed as,

$$|\psi\rangle \leftrightarrow F_\psi^*(z) := \sum_{n \geq 0} \frac{\psi^{(n)}}{\sqrt{n!}} z^n, \quad (11)$$

which is called the stellar function of the state $|\psi\rangle$. This stellar function corresponds to an expansion as a sum in the overcomplete basis of Glauber canonical coherent states [33]. Using the Hadamard-Weierstrass factorisation theorem, we can rewrite these stellar functions as

$$F_\psi^*(z) = e^{-\frac{1}{2}az^2+bz+c} z^k \prod_n \left(1 - \frac{z}{\lambda_n} \right) e^{\frac{z}{\lambda_n} + \frac{1}{2} \frac{z^2}{\lambda_n^2}}, \quad (12)$$

where the constants, $a, b, c, k, \lambda_n \in \mathbb{C}$ are each dependent on $|\psi\rangle$. Here, n is given as the so-called *stellar rank* of the function. For stellar functions of finite rank (i.e. finite roots of the polynomial, n), we can write our function as separable in Gaussian and polynomial functions as,

$$F_\psi^*(z) = G(z)P(z). \quad (13)$$

This decomposition can be written as,

$$F_\psi^\star(z) = e^{-a/2z^2+bz+c} \sum_{j=0}^N \beta_j z^j, \quad (14)$$

for $a, b, c, \beta_j \in \mathbb{C}$, which is the form that we will use in the remainder of the paper. Note that states with infinite rank, such as GKP [43] or cat states, are outside the stellar hierarchy and do not have an obvious measure of quantumness. However, they can be approximated with arbitrary precision using finite-rank states [44].

These stellar functions live in the Segal-Bargmann space, the separable infinite-dimensional Hilbert space of holomorphic functions F^\star over \mathbb{C}^m , satisfying the normalization condition,

$$\|F^\star\|^2 := \int_{\mathbf{z} \in \mathbb{C}^m} d^{2m}z \, e^{-|\mathbf{z}|^2} |F^\star(\mathbf{z})|^2 < +\infty, \quad (15)$$

which constrains $|\operatorname{Re}(a)| < 1$ in Eq. (14). The SB space has the inner product,

$$\langle F_1^\star | F_2^\star \rangle_{SB} = \int_{\mathbf{z} \in \mathbb{C}^m} d^{2m}z \, e^{-|\mathbf{z}|^2} F_1^\star(\mathbf{z})^* F_2^\star(\mathbf{z}). \quad (16)$$

In the SB space, our operators are functions of the creation and annihilation operators acting on the Hilbert space of our quantum states, and are mapped to differential operators in the SB space by,

$$\hat{a}^\dagger \leftrightarrow z \times \text{ and } \hat{a} \leftrightarrow \partial_z, \quad (17)$$

where $z \times$ acts on a holomorphic function by multiplying it by z and ∂_z takes the partial derivative of it with respect to z . It follows that any unitary evolution acting on an element of the SB space remains within the space. It is also understood that any unitary only changes the polynomial component of a stellar function and Gaussian unitary operations do not change the stellar rank at all.

The stellar functions in this space are described by their stellar rank (n): the number of polynomial roots they have. The key results of [33] and [34] prove that stellar rank provides a useful measure of classical simulability, a fact we later utilise to analyse the simulability of CV quantum kernels. Roughly, the measurement of a general non-separable, CV state $|\psi\rangle$ can be strongly simulated in time $O(2^n)$, where n is the stellar rank [34].

Common examples of zero stellar rank functions are vacuum states, coherent states, squeezed states and two-mode squeezed states. Fock states of n particle number have stellar rank n . Important properties of the stellar rank as a measure of non-Gaussianity include the fact that it is conserved under Gaussian operations, that the states of finite stellar rank form a dense subset of the SB space, and that operationally one can climb the hierarchy by acting on a given state with a creation operator (see Figure 1.).

We will next use these representations of CV quantum states to develop analytic representations of CV quantum kernels.

3.2 CV quantum feature maps

Given some metric space of our data \mathcal{X} we can define our CV holomorphic kernel as follows. Firstly, let us encode our data $\mathbf{x}_i \in \mathcal{X}$ to a pure quantum state which we then decompose into its Fock basis,

$$\mathbf{x}_i \rightarrow |\psi_{\mathbf{x}_i}\rangle = \sum_{n \geq 0} \psi_{\mathbf{x}_i}^{(n)} |n\rangle. \quad (18)$$

Using the transformation from equation 10 we yield,

$$|\psi_{x_i}\rangle \leftrightarrow F_{x_i}^*(z) := \sum_{n \geq 0} \frac{\psi_{x_i}^{(n)}}{\sqrt{n!}} z^n. \quad (19)$$

This allows our data to be encoded into some continuous variable state via holomorphic function, where we use the stellar rank as a notion of quantumness of the feature map, $|\psi_{x_i}\rangle$ – the higher the value of n , the more difficult the state is to classically simulate. This forms our data encoding,

$$x_i \mapsto \Phi(x_i) := F_{x_i}^*(z), \quad (20)$$

from which we define our kernel as,

$$k(x_1, x_2) = |\langle \psi(x_1) | \psi(x_2) \rangle|^2 = \left| \langle F_{x_1}^*(z) | F_{x_2}^*(z) \rangle_{SB} \right|^2. \quad (21)$$

This function is positive semi-definite and (appendix A) symmetric [2] and thus a valid kernel.

We can define the RKHS as the completion of the span of the kernel function for some data set \mathcal{X} . We see that the Segal-Bargmann space can be understood as the RKHS of the Gaussian kernel which itself is universal (appendix B).

4 Examples of single-mode CV quantum kernels

Before characterising a general form for arbitrary multi-mode CV quantum kernels we will first start with some simple examples. We first construct an analytic expression for a kernel generated from a displaced, single-mode Fock state encoding and show this kernel is rotationally and translationally invariant, radial and characteristic. We then derive an expression for the same state when one also encodes data into a phase shift—the resulting kernel is no longer translationally or rotationally invariant.

4.1 Displaced Fock state kernel

4.1.1 Closed form & analytic properties

We first consider a simple single-mode bosonic kernel which encodes data through a general Fock state $|n\rangle$ with an applied displacement unitary $\hat{D}(\alpha)|n\rangle$. To encode 2 pieces of information $\alpha = (\alpha_1, \alpha_2)^T \in \mathcal{X} \subset \mathbb{R}^2$, we parameterise the displacement operator by the complex number $\alpha := \alpha_1 + i\alpha_2$. This operator acts on any holomorphic function as

$$F^*(z) \mapsto e^{\alpha z - |\alpha|^2/2} F^*(z - \alpha^*). \quad (22)$$

Since displacement is a Gaussian operation, it will not change the stellar rank of $F^*(z)$; therefore the encoded state $\hat{D}(\alpha)|n\rangle$ will have a stellar rank of n . Explicitly, the encoded state is

$$\hat{D}(\alpha)|n\rangle \leftrightarrow F_\alpha^*(z) = e^{\alpha z - |\alpha|^2/2} \frac{(z - \alpha^*)^n}{\sqrt{n!}} \quad (23)$$

and with this encoding, the quantum kernel is

$$k(\alpha, \beta) = \left| \langle F_\alpha^*(z) | F_\beta^*(z) \rangle \right|^2 \quad (24)$$

where

$$\begin{aligned} \langle F_\alpha^\star(z) | F_\beta^\star(z) \rangle &= \int_{z \in \mathbb{C}} d^2z \, e^{-|z|} (F_\alpha^\star(z))^* F_\beta^\star(z) \\ &= \frac{1}{\pi} \frac{e^{-(|\alpha|^2 + |\beta|^2)/2}}{n!} \int_{z \in \mathbb{C}} d^2z \, e^{-(|z|^2 - \alpha^* z^* - \beta z)} (z^* - \alpha)^n (z - \beta^*)^n. \end{aligned} \quad (25)$$

After the integration and some algebra (see appendix D for details), we can write down the displacement kernel in closed form as:

$$\begin{aligned} k_D(\alpha, \beta) &= \left| \langle F_\alpha^\star(z) | F_\beta^\star(z) \rangle \right|^2 \\ &= \left(\frac{n!}{\pi} \right)^2 e^{-|\alpha - \beta|^2} \left| \sum_{i=0}^n \sum_{j=0}^{n-i} \sum_{k=0}^n \sum_{\ell=0}^{n-k} \sum_{p=0}^{i+k} \sum_{q=0}^{j+\ell} \frac{(-i)^j (-\alpha)^{n-i-j}}{i! j! (n-i-j)!} \frac{(i)^\ell (-\beta^*)^{n-k-\ell}}{k! \ell! (n-k-\ell)!} \right. \\ &\quad \left. \times \gamma_{(i+k), p} \gamma_{(j+\ell), q} (\alpha^* + \beta)^p (-i(\alpha^* - \beta))^q \right|^2 \end{aligned} \quad (26)$$

where

$$\gamma_{r,j} := \begin{cases} \Gamma\left(\frac{1}{2} + \frac{r}{2}\right) \frac{(r/2)!}{2^{j/2} (1/2)_{j/2}}, & r, j \text{ even} \\ \Gamma\left(\frac{3}{2} + \frac{r-1}{2}\right) \frac{((r-1)/2)!}{2^{j/2} (3/2)_{(j-1)/2}}, & r, j \text{ odd} \\ 0, & \text{otherwise} \end{cases} \quad (27)$$

are constants, which depend on the integer values of $r \geq 0$ and $j \leq r$, and $(x)_j$ is the Pochhammer symbol. In appendix D.2, we list the explicit form of this kernel for the first 9 Fock states.

From Eq. (26), it is clear that the displacement kernel is the product of a Gaussian and a polynomial of degree $4n$ in both α and β , because

$$\begin{aligned} 2(i+k+j+\ell+(n-i-j)) &= 2(n+k+\ell) \\ &\xrightarrow[\ell]{\max} 2(n+k+(n-k)) = 4n \\ 2(i+k+j+\ell+(n-k-\ell)) &= 2(n+i+j) \\ &\xrightarrow[j]{\max} 2(n+i+(n-i)) = 4n \end{aligned}$$

Using this closed form expression we are also able to show that the kernel is translation (shift) and rotation invariant (see appendices D.3 and D.4). From these properties, we find that (see appendix D.5)

$$k(\alpha, \beta) = k(|\alpha - \beta|), \quad (28)$$

and so it is a radial kernel. This combined with the fact that the Fourier transform of this kernel is also the product of a Gaussian and a polynomial of degree $4n$, which has support over the entire Fourier domain, except at a finite number of points (see appendix D.6), means that the displaced Fock state kernel is a characteristic kernel [45].

In order to generate some intuition as to how such a kernel will behave, in figure 2 we plot the displaced Fock state kernel function, $k(|\alpha - \beta|)$, for training data chosen from a uniform distribution of $|\alpha - \beta|$ from 0 to 8, for various values of the stellar rank, n . We see in the figure that as the value of n increases, so does the number of zeros in the kernel function, as expected. Additionally, as the stellar rank increases, the kernel's ability to distinguish between large distances in the original data space, $|\alpha - \beta|$, improves. For

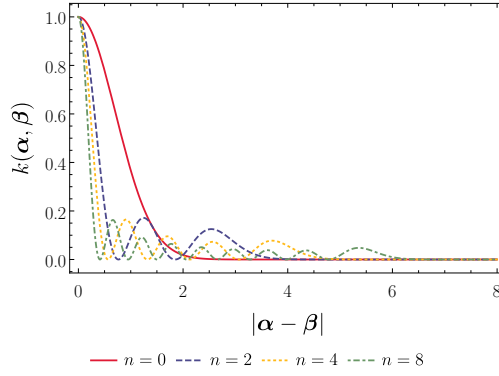


Figure 2: The kernel function in the case of displacement encoding (Eq. (23)) as a function of $|\alpha - \beta|$, the distance in the data space, for various values of the initial Fock state, n .

example, the $n = 2$ kernel function will evaluate as zero for any distance $|\alpha - \beta|$ greater than 4, whereas the $n = 8$ kernel will have non-zero values up to a distance of 6.

We can also see that for kernels of finite stellar rank, due to multiplication by the Gaussian factor $e^{-|\alpha - \beta|^2}$, there will be a threshold value beyond which all kernel evaluations will be exponentially close to zero. Additionally, it appears that as stellar rank increases, the amplitudes of the maxima diminish. This would suggest that as the stellar rank increases, kernel values outside the central peak will become increasingly suppressed. This is further supported by the fact that the displaced Fock state kernels integrate to a constant value, π (appendix D.7), which limits how large each maximum can be. Given these two results, we would expect, therefore, that displaced Fock state CV kernels of high stellar rank will generate kernel values that are increasingly concentrated at low values, a feature that we observe in the learning experiments conducted below. Given kernel values are always statistically approximated by repeated measurement, as kernel values become smaller they require more measurements to remain distinguishable. Consequently, we expect high stellar rank models with low kernel variance will also become increasingly vulnerable to shot noise.

4.1.2 Bandwidth tuning

This observation has some of the flavour of exponential concentration and recent work has proposed bandwidth tuning as a possible mitigation technique [24]. Let us therefore consider the consequences of implementing a bandwidth c on the encoded data by taking

$$\alpha \rightarrow c\alpha, \quad (29)$$

where $c > 0$ is a real hyperparameter. Physically, this corresponds to a reduction in the value of the displacement of the Fock state, $\hat{D}(\alpha)|n\rangle \rightarrow \hat{D}(c\alpha)|n\rangle$, which results in a non-linear transformation of the kernel.

In figure 3, we explore the effect of the bandwidth c on the value of the displaced Fock state kernel function. We take some data, which we choose to be a uniform distribution of $|\alpha - \beta|$ from 0 to 6, and apply a bandwidth so that

$$|\alpha - \beta| \rightarrow |c\alpha - c\beta| = c|\alpha - \beta|. \quad (30)$$

We find that for this particular choice of distribution, a bandwidth of $c = 0.5$ moves all of the data away from the tail of the function (where values are exponentially close to zero). For example, all data separated in the original space by values > 5 but < 6 have kernel

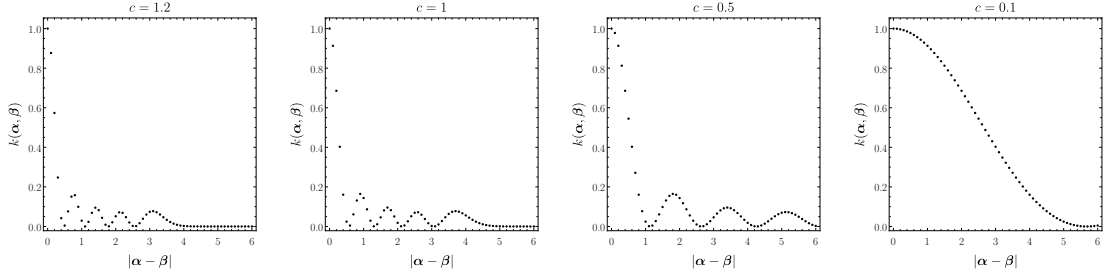


Figure 3: The kernel function in the case of displacement encoding (Eq. (23)) with $n = 4$ for a uniform distribution of $|\alpha - \beta| \in [0, 6]$ for various values of the bandwidth hyperparameter set to, from left to right, $c = 1.2$, $c = 1$, $c = 0.5$, $c = 0.1$.

values of near zero for $c = 1$ (left figure) but for a bandwidth of $c = 0.5$, we can see these data points can now be discriminated. Unfortunately, it is also the case that data points that were easily distinguishable for $c = 1$, such as the two points closest to the y axis, are less distinguishable following bandwidth tuning to $c = 0.5$. Furthermore, we also see that this bandwidth reduces the *effective* stellar rank of the kernel function, since there are now only $n = 4$ maxima, rather than $n = 5$ over the range of the distribution (although we note that the actual stellar rank of the kernel function does not change, since it is still defined for all $|\alpha - \beta| \in [0, \infty)$). On the other hand, a bandwidth is 1.2, moves more of the data into the tail of the function as compared with no bandwidth, exponentially suppressing data with values larger than ~ 4 . In the case of a very small bandwidth, $c = 0.1$, the kernel function is effectively a Gaussian, and consequently classically simulable. In conclusion, it is reasonable to expect that the hyperparameter, c will need to be carefully chosen for each problem.

4.1.3 Learning experiments

In this section we present some performance metrics and decision boundaries for implementations of a range of displaced Fock state kernels. We create a task to exploit the underlying structure of the displaced Fock state kernel. The task is a supervised learning classification task using an annular data set constructed by combining multiple instances of the Scikit-learn data set method, *make circles*. We combine 3 instances of the method, each with different parameters to yield 3 concentric circles of data with binary labels. We define 500 data points in the data set for each set of circles, and an equal number for each label $\{0, 1\}$. We create three data sets: one with circles that are close together and a small amount of noise (0.05), one which modifies the first by flipping the labels above the $y = 0$ axis, and one which modifies the first by increasing the separation between the circles and adding more noise (0.3). The three data sets are illustrated in figure 4. When we increase the separation between the circles in the third data set, we maintain the ratios of radii of the blue and red circles as 0.3 for the inner circles, 0.8 for the middle circles and 0.9 for the outer circles. In all three learning simulations, the train-test split is the default 75%, 25% split.

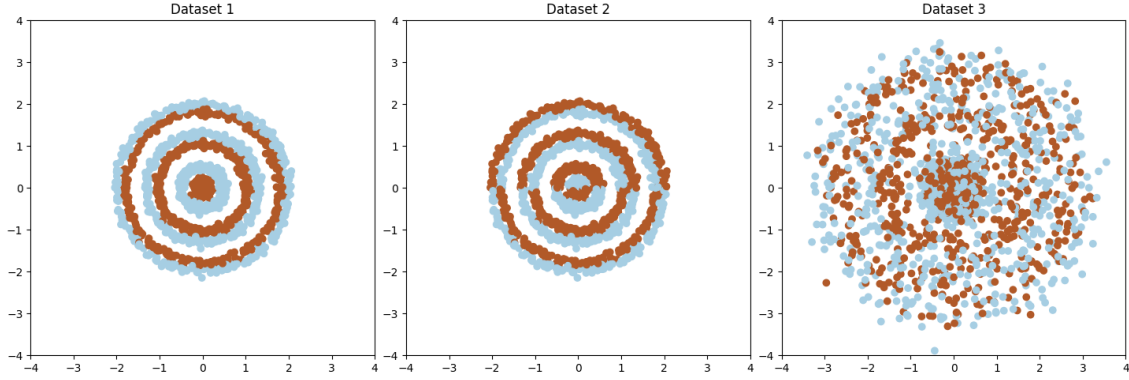


Figure 4: Data set 1 (*left*) includes tightly packed circles with little added noise while data set 3 (*right*) has circles with larger separation and substantially more noise. Data set 2 (*centre*) is a modification of data set 1 where labels above $y = 0$ are flipped, which adds more complexity to the data.

First, we test on data set 1. In figure 5 we plot the test data and decision boundaries and accuracy for five kernels, three displaced Fock state kernels with $n = 1, 2, 3$, the Scikit-learn Gaussian kernel without hyperparameter tuning and the same Gaussian kernel which has been tuned using Bayesian optimization. We do not perform any tuning on the displaced Fock state kernels. We see that the accuracy of the displaced Fock state kernels improves with increasing stellar rank (first three panels) and the $n = 2$ and $n = 3$ kernels significantly outperform the default classical Gaussian kernel (fourth panel). However, when the Gaussian kernel has been tuned, it is also able to classify the data to a high degree of accuracy (fifth panel). Tuning the Gaussian kernel via Bayesian optimisation to achieve this accuracy takes a significant amount of computational time, while the displaced Fock state kernels require no hyperparameter tuning, suggesting that these quantum kernels are better suited for this task.

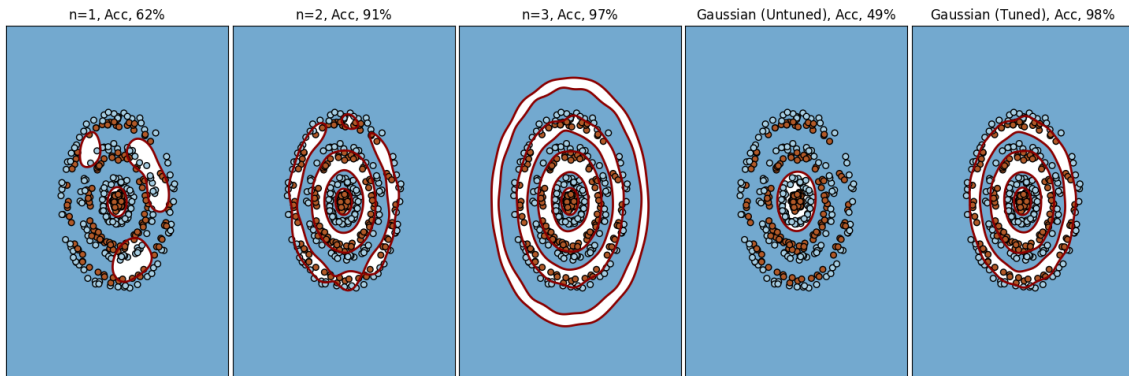


Figure 5: Plots of the decision boundaries for $n = 1, 2, 3$ displaced Fock state kernels (left three panels) with no hyperparameter tuning, benchmarked against a classical Gaussian kernel (right two panels) for data set 1. As this annular data is constructed from close circles, we see that accuracy increases with stellar rank as higher rank kernels can identify finer structure. On this particular problem, the quantum displaced Fock state kernels outperform the Scikit-learn Gaussian kernel with default hyperparameters. When the Gaussian kernel is tuned using Bayesian optimisation, it can fit the data to a much higher accuracy than when it is untuned.

In data set 2, we add an additional complexity by flipping the labels in data set 1 above the $y = 0$ axis, and again test on five kernels: the displaced Fock state kernel with stellar

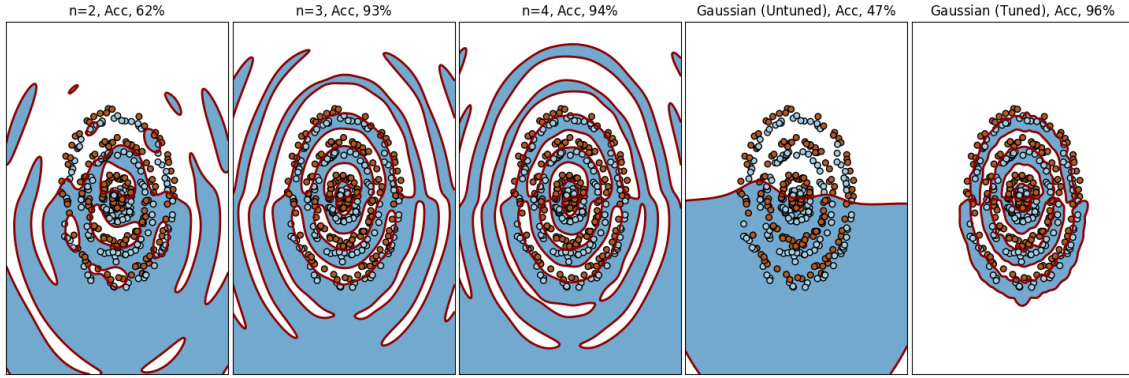


Figure 6: Plots of the decision boundaries for $n = 2, 3, 4$ displaced Fock state kernels (left three panels) with no hyperparameter tuning, benchmarked against a classical Gaussian kernel (right two panels) for data set 2. The accuracy increases with stellar rank. The quantum displaced Fock state kernels outperform the Scikit-learn Gaussian kernel with default hyperparameters; however, after the Gaussian kernel is tuned using Bayesian optimisation, it can fit the data to a much higher accuracy than when it is untuned.

rank $n = 2, 3, 4$ with no hyperparameter tuning, and the Gaussian kernel without and with hyperparameter tuning. The decision boundaries, test data and accuracy of these kernels is plotted in figure 6. Similar to the tests on data set 1, we find that the accuracy of the displaced Fock state kernels improves with increasing stellar rank (first three panels), since higher stellar rank kernels can identify finer structure. In particular, the $n = 3$ and $n = 4$ kernels were well suited for this learning task. The $n = 1$ kernel had very poor accuracy, so it was omitted from this figure. We also found that the Gaussian kernel also performed well, but again only after tuning via computationally expensive Bayesian optimisation (fourth and fifth panel), suggesting it is less suited for such a classification task.

Next, we consider the effect of the bandwidth hyperparameter on the displaced Fock state kernels. In figure 7, we use data set 1 to determine the effect of the bandwidth on the accuracy of the $n = 1$ displaced Fock state kernel, which under-fits the data. Increasing the bandwidth from 1 to 1.5 results in an improvement in accuracy from 62% to 97%. However, increasing bandwidth to 15 results in over-fitting and test accuracy starts to decline again.

In figure 8 we use data set 3 to determine how the bandwidth affects generalisation for noisy data. We see that for the $n = 3$ while bandwidth tuning can improve the performance from 60% to 63%, the decision boundary becomes closer to that of a lower rank kernel (last panel). Continued bandwidth tuning eventually results in a kernel that approximates an un-tuned Gaussian kernel. This corroborates the theoretical behaviour we illustrated in figure 3: decreasing the bandwidth decreases the effective stellar rank of the kernel.

Overall, these learning simulations demonstrate the displaced Fock state CV kernel is well suited to learn on data sets whose structure matches the structure of kernel function (e.g. annular data). Additionally, tuning the bandwidth hyperparameter can improve accuracy if the model is under-fit, or the data is noisy.

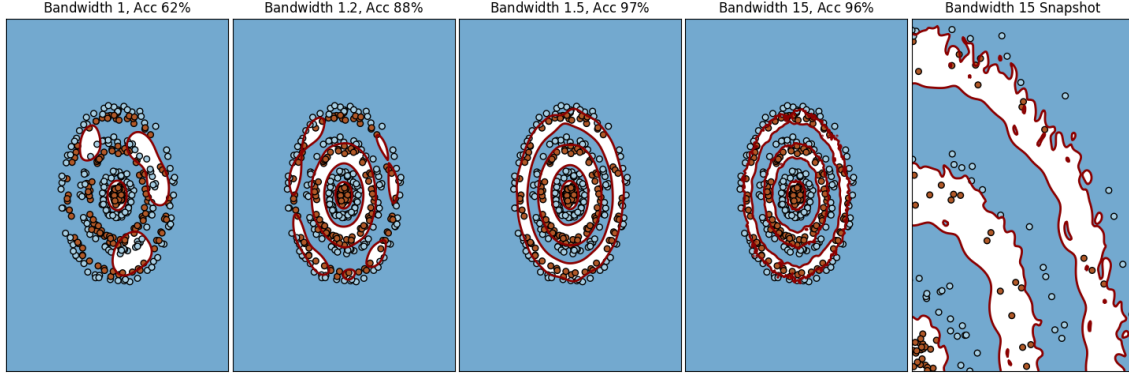


Figure 7: Here we use data set 1 and plot the performance of the $n = 1$ displaced Fock state kernel. Tuning the bandwidth hyperparameter permits the kernel to learn the finer grained detail of the data and will improve the performance of an underfit model. However, further tuning of bandwidth can eventually result in a model that is overfit (right-most panel).

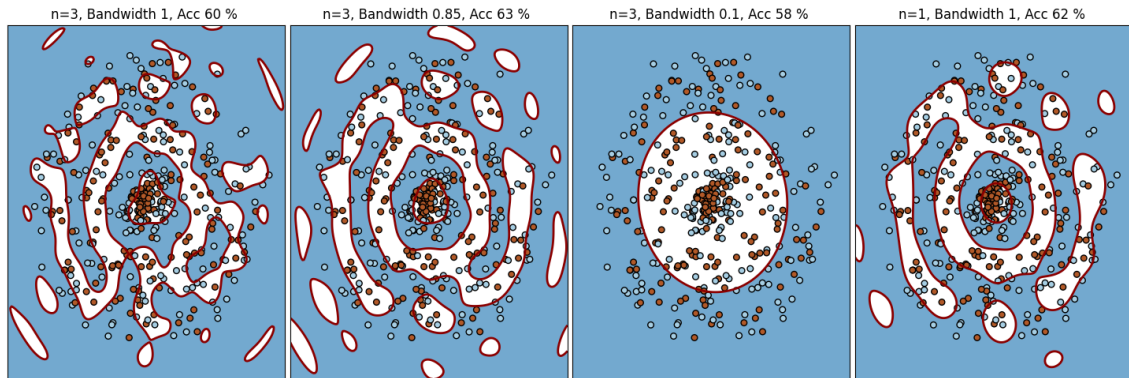


Figure 8: In the case where data is noisy, with wider and further separated circles, we test the $n = 3$ kernel against 3 values of bandwidth. We see that reducing the bandwidth can take an over-fit kernel (panel 1) to one which generalises better (panel 2). The tradeoff, however, is that the decision boundary now closely resembles one for the lower rank $n = 1$ kernel (panel 4). Again, further tuning leads to a Gaussian kernel (panel 3).

4.2 Displacement-phase encoding

The single-mode displaced Fock state encoding only permits encoding of two dimensional data. In this subsection we evaluate a single-mode CV kernel that permits encoding of three dimensional data.

Another Gaussian operator is the phase shift operator, $\hat{R}(\varphi)$, which acts on a holomorphic function as

$$F^*(z) \mapsto F^*(e^{i\varphi}z). \quad (31)$$

We will apply this, along with the displacement operator to a Fock state $|n\rangle$ to encode a third number, $0 \leq \varphi < 2\pi$, so that now

$$\boldsymbol{\alpha} = (\alpha_1, \alpha_2, \varphi)^T \in \mathcal{X} \subset \mathbb{R}^2 \times [0, 2\pi). \quad (32)$$

If the phase operator acts on the Fock state before the displacement operator,

$$\begin{aligned} \hat{D}(\alpha)\hat{R}(\varphi)|n\rangle &\rightarrow \hat{D}(\alpha)\frac{(e^{i\varphi}z)^n}{\sqrt{n!}} = e^{\alpha z - |\alpha|^2/2} \frac{(e^{i\varphi}(z - \alpha^*))^n}{\sqrt{n!}} \\ &= e^{i\varphi} e^{\alpha z - |\alpha|^2/2} \frac{(z - \alpha^*)^n}{\sqrt{n!}} \\ &= e^{i\varphi} \hat{D}(\alpha)|n\rangle \end{aligned} \quad (33)$$

the resulting holomorphic function differs from the displaced Fock state encoding Eq. (23) only by a phase. Therefore, a kernel with this encoding will reduce to the displaced Fock state kernel, i.e.

$$\left| \langle n | \hat{R}^\dagger(\varphi) \hat{D}^\dagger(\alpha) \hat{D}(\beta) \hat{R}(\vartheta) | n \rangle \right|^2 = \left| \langle n | \hat{D}^\dagger(\alpha) \hat{D}(\beta) | n \rangle \right|^2. \quad (34)$$

Alternatively, we can apply displacement operator to a Fock state $|n\rangle$, followed by a phase shift operator

$$\begin{aligned} \hat{R}(\varphi)\hat{D}(\alpha)|n\rangle &\rightarrow \hat{R}(\varphi) e^{\alpha z - |\alpha|^2/2} \frac{(z - \alpha^*)^n}{\sqrt{n!}} \\ &= \exp\left(e^{i\varphi}\alpha z - \frac{|\alpha|^2}{2}\right) \frac{(e^{i\varphi}z - \alpha^*)^n}{\sqrt{n!}}. \end{aligned} \quad (35)$$

as the encoding of $\boldsymbol{\alpha}$.

With this encoding, the kernel is easy to calculate by noting that taking $\alpha \rightarrow e^{i\varphi}\alpha$ in Eq. (33) results in Eq. (35), and so applying this transformation to Eq. (26), results in the phase-displacement kernel:

$$\begin{aligned} k_{RD}(\boldsymbol{\alpha}, \boldsymbol{\beta}) &= \left| \langle F_{\alpha, \varphi}^*(z) | F_{\beta, \vartheta}^*(z) \rangle \right|^2 \\ &= \left(\frac{n!}{\pi} \right)^2 e^{-|\alpha - \beta|^2} \left| \sum_{i=0}^n \sum_{j=0}^{n-i} \sum_{k=0}^n \sum_{\ell=0}^{n-k} \sum_{p=0}^{i+k} \sum_{q=0}^{j+\ell} \frac{(-i)^j e^{i(n-i-j)\varphi} (-\alpha)^{n-i-j}}{i!j!(n-i-j)!} \right. \\ &\quad \times \frac{(i)^\ell e^{-i(n-p-q)\vartheta} (-\beta^*)^{n-k-\ell}}{k!\ell!(n-k-\ell)!} \gamma_{(i+k), p} \gamma_{(j+\ell), q} \\ &\quad \left. \times (e^{-i\varphi}\alpha^* + e^{i\vartheta}\beta)^p (-i(e^{-i\varphi}\alpha^* - e^{i\vartheta}\beta))^q \right|^2 \end{aligned} \quad (36)$$

where $\gamma_{r,j}$ is defined in Eq. (27).

Unlike the displaced Fock state kernel, the phase-displacement kernel is not, in general, translation invariant. Consider the example of $n = 1$, where

$$\begin{aligned} \langle F_{\alpha,\varphi}^*(z) | F_{\beta,\vartheta}^*(z) \rangle &= \exp\left(-\frac{|\alpha|^2 + |\beta|^2}{2}\right) \exp\left(e^{i(\vartheta-\varphi)} \alpha^* \beta\right) \exp(i(\vartheta - \varphi)) \\ &\times \left[1 - |\alpha|^2 - |\beta|^2 + 2 \operatorname{Re}\left(e^{i(\vartheta-\varphi)} \alpha^* \beta\right)\right] \end{aligned} \quad (37)$$

and apply a translation of $\mathbf{h} = (h_1, h_2, \eta)^\top$, where $h_1, h_2 \in \mathbb{R}$ and $\eta \in [0, 2\pi)$. Additionally, define $h = h_1 + ih_2$, so the shifted kernel is:

$$k_{RD}(\boldsymbol{\alpha} + \mathbf{h}, \boldsymbol{\beta} + \mathbf{h}) = \left| \langle F_{\alpha+h, \varphi+\eta}^*(z) | F_{\beta+h, \vartheta+\eta}^*(z) \rangle \right|^2 \quad (38)$$

where

$$\begin{aligned} &\langle F_{\alpha+h, \varphi+\eta}^*(z) | F_{\beta+h, \vartheta+\eta}^*(z) \rangle \\ &= \exp\left(-\frac{|\alpha|^2 + |\beta|^2}{2}\right) \exp\left(e^{i(\vartheta-\varphi)} \alpha^* \beta\right) \exp\left(i \operatorname{Im}(h(\alpha^* - \beta^*))\right) \\ &\times \exp\left((e^{i(\vartheta-\varphi)} - 1)(|h|^2 + h\alpha^* + h^*\beta)\right) \exp(i(\vartheta - \varphi)) \\ &\times \left[1 - |\alpha|^2 - |\beta|^2 + 2 \operatorname{Re}\left(e^{i(\vartheta-\varphi)} \alpha^* \beta\right) + 2 \operatorname{Re}\left((e^{i(\vartheta-\varphi)} - 1)(h\alpha^* + h^*\beta)\right) \right. \\ &\quad \left. - 4|h|^2 \sin^2\left(\frac{\vartheta - \varphi}{2}\right)\right]. \end{aligned} \quad (39)$$

This clearly depends on \mathbf{h} by more than an overall phase, so the kernel will also be dependent on \mathbf{h} .

Since this kernel is not shift invariant

$$k_{RD}(\boldsymbol{\alpha}, \boldsymbol{\beta}) \neq k_{RD}(\boldsymbol{\alpha} - \boldsymbol{\beta}), \quad (40)$$

it is a function of all five encoded parameters: $\alpha_1, \alpha_2, \beta_1, \beta_2$ and the phase difference $(\vartheta - \varphi)$. However, on closer examination, we find that most of the complexity of the resulting kernel can be captured by the phase shift. In figure 9 we explore this additional complexity, by plotting the kernel function as a function of two encoded variables, α_1 and β_1 for various values of $(\vartheta - \varphi)$ and a fixed value of α_2 and β_2 . In all four figures, we find similar behaviour of the kernel; there is an overall elliptical profile with six maxima and five minima, corresponding to the stellar rank of $n = 5$. Additionally, the Gaussian part of the kernel again exponentially suppresses kernel values that are sufficiently far from the maximum. The overall eccentricity of the envelope depends on the phase difference. We find similar behaviour for the kernel function plotted as a function of α_2 and β_2 as well as plotted as a function of α_1 and β_2 .

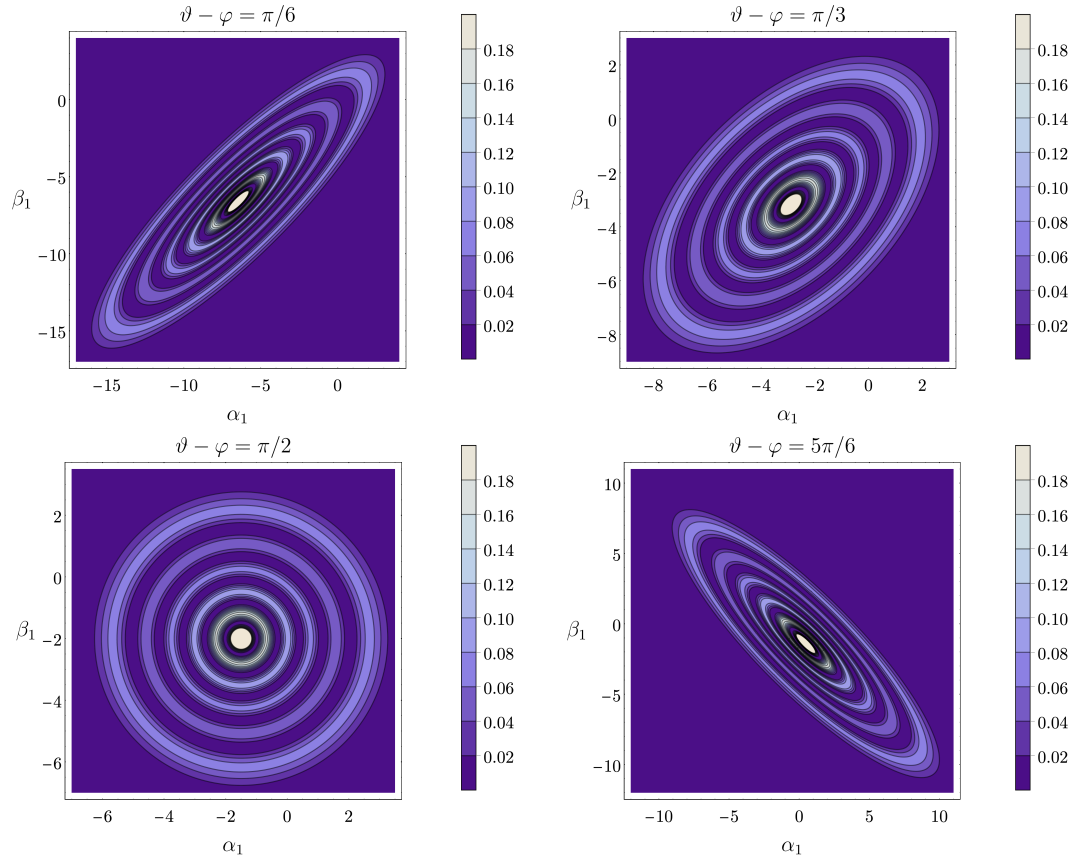


Figure 9: Here we depict two dimensional slices of the five dimensional kernel function in the case of displacement and phase shift encoding (Eq. (33)) with $n = 5$ as a function of the encoded real parameters α_1 and β_1 for the various values of the encoded: (top left) $\vartheta - \varphi = \pi/6$, (top right) $\vartheta - \varphi = \pi/3$, (bottom left) $\vartheta - \varphi = \pi/2$ and (bottom right) $\vartheta - \varphi = 5\pi/6$. The remaining real parameters are set to $\alpha_2 = -2$ and $\beta_2 = 1.5$.

5 General CV kernels

We have now provided some intuition for the behaviour of two simple CV kernel building blocks. It is clear, however, that it is unlikely that kernels which only encode data of two or three dimensions will have much utility. We therefore now consider kernels created via multi-mode states to enable the encoding of high dimensional data. A first challenge is to understand if we can still write such kernels in closed form.

A general m -mode state of total stellar rank n can be represented by the holomorphic function

$$F^\star(\mathbf{z}) = G(\mathbf{z})P(\mathbf{z}) \quad (41)$$

where $\mathbf{z} = (z_1, z_2, \dots, z_m)^\top$, $G(\mathbf{z})$ is a Gaussian and $P(\mathbf{z})$ is a polynomial [33].

In general,

$$\begin{aligned} G(\mathbf{z}) &= \exp\left(-\frac{1}{2}\mathbf{z}^\top \mathbf{A} \mathbf{z} + \mathbf{B}^\top \mathbf{z} + C\right) \\ P(\mathbf{z}) &= \sum_{\substack{i_1, i_2, \dots, i_m \geq 0 \\ i_1 + i_2 + \dots + i_m = n}} \beta_{\mathbf{i}} z_1^{i_1} z_2^{i_2} \dots z_m^{i_m} \end{aligned} \quad (42)$$

where $\mathbf{A} \in \mathbb{C}^m \times \mathbb{C}^m$ with components $A_{i,j}$ and $|\operatorname{Re}(A_{j,j})| < 1$, $\mathbf{B} \in \mathbb{C}^m$ with components B_j , $\mathbf{i} := (i_1, i_2, \dots, i_m)$, and $C, \beta_{\mathbf{i}} \in \mathbb{C}$. The actual values of these components will depend on the particular choice of feature map, which in general will be exponentially difficult to classically simulate for large values of n .

Given some encoding of data $\mathbf{x}_1, \mathbf{x}_2 \in \mathcal{X}$ into such a state, the quantum kernel is

$$k(\mathbf{x}_1, \mathbf{x}_2) = |\langle F_{\mathbf{x}_1}^\star | F_{\mathbf{x}_2}^\star \rangle|^2 \quad (43)$$

where

$$\begin{aligned} \langle F_{\mathbf{x}_1}^\star | F_{\mathbf{x}_2}^\star \rangle &= \frac{1}{\pi^m} \int_{\mathbf{z} \in \mathbb{C}^m} d^{2m}z \, e^{-|\mathbf{z}|^2} F_{\mathbf{x}_1}(\mathbf{z})^* F_{\mathbf{x}_2}(\mathbf{z}) \\ &= \frac{1}{\pi^m} \int_{\mathbf{z} \in \mathbb{C}^m} d^{2m}z \, e^{-|\mathbf{z}|^2} \exp\left(-\frac{1}{2}\mathbf{z}^\dagger \mathbf{A}^{(1)*} \mathbf{z}^* + \mathbf{B}^{(1)\dagger} \mathbf{z}^* + C^{(1)*}\right) \\ &\quad \times \left(\sum_{i_1 + i_2 + \dots + i_m = n} \beta_{\mathbf{i}}^{(1)*} (z_1^*)^{i_1} (z_2^*)^{i_2} \dots (z_m^*)^{i_m} \right) \\ &\quad \times \exp\left(-\frac{1}{2}\mathbf{z}^\top \mathbf{A}^{(2)} \mathbf{z} + \mathbf{B}^{(2)\top} \mathbf{z} + C^{(2)}\right) \left(\sum_{j_1 + j_2 + \dots + j_m = n} \beta_{\mathbf{j}}^{(2)} z_1^{j_1} z_2^{j_2} \dots z_m^{j_m} \right) \end{aligned} \quad (44)$$

and the superscripts keep track of the encoded data.

Calculating this inner product (see appendix C.1) requires the evaluation of $2m$ integrals, each of the form

$$\begin{aligned} I_r(a, b) &:= \int_{-\infty}^{\infty} dx \, \exp(-ax^2 + bx) x^r \\ &= a^{-(r+1)/2} \exp\left(\frac{b^2}{4a}\right) \sum_{j=0}^r \gamma_{r,j} \left(\frac{b}{\sqrt{a}}\right)^j \end{aligned} \quad (45)$$

where the $\gamma_{r,j}$'s are defined in Eq. (27). This can be done algorithmically, (see appendix E), and we are able to obtain a closed form expression for the general m -mode kernel

$$\begin{aligned} \langle F_{x_1}^* | F_{x_2}^* \rangle &= \frac{1}{\pi^m} \exp \left(C^{(1)*} + C^{(2)} + \sum_{j=1}^{2m} \frac{b_{j-1,j}^2}{4a_{j-1,j}} \right) \sum_{i_1+\dots+i_m=n} \sum_{j_1+\dots+j_m=n} \beta_i^{(1)*} \beta_j^{(2)} \\ &\times \sum_{p=0}^i \sum_{q=0}^j \prod_{\ell=1}^{2m-1} \left(\sum_{s_\ell=0}^{r_{\ell-1,\ell}} \frac{\gamma_{r_{\ell-1,\ell},s_\ell}}{a_{\ell-1,\ell}^{(r_{\ell-1,\ell}+s_\ell+1)/2}} \sum_{t_\ell=0}^{s_\ell} \frac{s_\ell!}{(s_\ell-t_\ell)!} b_{\ell-1,\ell}^{s_\ell-t_\ell} \right. \\ &\times \left. \sum_{u_{\ell,\ell+1}+\dots+u_{\ell,2m}=t_\ell} g_{\ell,\ell+1} \right) \left(\sum_{s_{2m}=0}^{r_{2m-1,2m}} \frac{\gamma_{r_{2m-1,2m},s_{2m}}}{a_{2m-1,2m}^{(r_{2m-1,2m}+s_{2m}+1)/2}} b_{2m-1,2m}^{s_{2m}} \right) \end{aligned} \quad (46)$$

where a , b , d , g , and r are defined recursively as

$$\begin{aligned} a_{i,j} &:= a_{i-1,j} - \frac{d_{i-1,i,j}^2}{4a_{i-1,j}} \\ b_{i,j} &:= b_{i-1,j} + \frac{b_{i-1,i}d_{i-1,i,j}}{2a_{i-1,i}} \\ d_{i,j,k} &:= d_{i-1,j,k} + \frac{d_{i-1,i,j}d_{i-1,i,k}}{2a_{i-1,i}} \end{aligned} \quad (47)$$

which depend, in part, on the initial encoding of x_1 and x_2 and

$$\begin{aligned} g_{i,k} &:= \frac{g_{i-1,k}d_{i-1,i,k}^{u_{i,k}}}{u_{i,k}!} \\ r_{i,k} &:= r_{i-1,k} + u_{i,k}. \end{aligned} \quad (48)$$

The initial values of these parameters are defined in appendix E.

While the detail of this kernel function is opaque, we note that any CV encoding of a finite stellar rank will always have a kernel of the form of Eq. (46), and can be expressed as a product of a Gaussian and an algebraic function. Specifically, the algebraic function is a solution to the polynomial equation of the form $P_0(\mathbf{x}) = P_2(\mathbf{x})f(\mathbf{x})^2$. Furthermore, as the modulus squared of the inner product between two physically encoded CV quantum states is always bounded between 0 and 1, this means the kernel is always finite. Mathematically, we can also see this by noting that Eqs. (41) and (42) are defined on the SB space, the inner product is bounded.

Given this structure, we would expect to see similar behaviour as in the single-mode examples given in section 4. The Gaussian term will cause exponential suppression of kernel values beyond a certain threshold, and while this threshold can be manipulated by bandwidth tuning, this will most likely be at the cost of effective stellar rank. Again, we stress that these are general observations and the details will differ for each specific encoding. Additionally, we show in appendix F that CV encoding of an infinite stellar rank can be approximated arbitrarily well by kernels of this form. In the case where the matrix $\mathbf{A} = \mathbf{0}$ in Eq. (42), then the algebraic function in Eq. (46) will reduce to polynomial of degree $4n$ (since all $a_{i,j} = 1$ and $d_{i,j,k} = 0$). Some examples include the displaced Fock state (section 4.1) and displacement-phase encoding (section 4.2) as well as for the qudit kernel which we will detail in section 6. CV kernels of this form, expressed as the product of a Gaussian and a polynomial, are also holomorphic functions of finite stellar rank, thus

according to [34], the strong classical simulability of such kernels will scale exponentially on the order of $\mathcal{O}(2^{4n})$.

It remains an open question as to how the simulability of the general CV kernel function with $\mathbf{A} \neq \mathbf{0}$ will scale with n . However, we can gain some insight here by observing that in Eq. (46) classically simulating the kernel also scales exponentially in m , the mode of the encoding, given that $m \leq n$. The scaling with m comes from the general form within the product of sums,

$$\prod_{l=1}^{2m-1} (\dots), \quad (49)$$

representing a deeply nested sum of depth $2m - 1$. Each of the sums within this product are dependent on the index of prior sums and the total length of each sum also increases as a function of m . It can be easily seen that the computational complexity of m nested sums each of length $\geq l$ scales as $\mathcal{O}(l^m)$. As such, we see that our general kernel's classical simulability scales as at least $\mathcal{O}(l^m)$ for some $l > 1$ which we can fix.

This is a useful property as in practice the easiest way of increasing the stellar rank, and hence the complexity, of a CV quantum feature map is to increase the number of modes rather than directly increasing the stellar rank of a single mode.

6 Qudit kernels

Thus far we have only examined the CV case and it is interesting to ask if any of our results are applicable in the more familiar discrete qubit/qudit case. In fact, qudits of dimension d can also be represented as complex polynomials in the SB space as [33]

$$|\psi\rangle = \sum_{j=0}^{d-1} \alpha_j |j\rangle \rightarrow F_\psi^*(z) = \sum_{j=0}^{d-1} n_{d,j} \alpha_j z^j \quad (50)$$

where $n_{d,j} \in \mathbb{C}$ is a normalization factor, which only depends on d and j and ensures that

$$\langle F_\psi^*(z) | F_\psi^*(z) \rangle_{SB} = \sum_{j=0}^{d-1} |\alpha_j|^2 = 1. \quad (51)$$

We note that a tensor product of m qudits, each of dimension d , can always be written as a single qudit of dimension $m \times d$, so we will only consider the single-mode case.

As with the CV kernels, we consider the qudit kernel to be

$$k(\mathbf{x}_1, \mathbf{x}_2) = |\langle \psi(\mathbf{x}_1) | \psi(\mathbf{x}_2) \rangle|^2 \quad (52)$$

where the data $\mathbf{x}_1, \mathbf{x}_2 \in \mathcal{X}$ are encoded into the states $|\psi(\mathbf{x}_1)\rangle$ and $|\psi(\mathbf{x}_2)\rangle$ respectively. In the case of mixed states, where the data is encoded into a density matrix $\hat{\rho}(\mathbf{x}) \in \mathbb{C}^d \otimes \mathbb{C}^d$, we will consider the vectorisation, which stacks the columns of the matrix to form a single vector $|\rho(\mathbf{x})\rangle \in \mathbb{C}^{2d}$ [1]. The vectorised state can then be represented as Eq. (50).

With the encoded qudits represented as polynomials in the SB space, we can calculate

the inner product as (see appendix G):

$$\begin{aligned}
\langle \psi(x_1) | \psi(x_2) \rangle &\rightarrow \langle F_1^*(z) | F_2^*(z) \rangle \\
&= \frac{1}{\pi} \int_{z \in \mathbb{C}} d^2 z \, e^{-z^2} \left(\sum_{i=0}^{d-1} n_{d,i}^* \alpha_i^{(1)*} (z^*)^i \right) \left(\sum_{j=0}^{d-1} n_{d,j} \alpha_j^{(2)} z^j \right) \\
&= \sum_{i=0}^{d-1} \sum_{j=0}^{d-1} \frac{1 + (-1)^{i+j}}{2} \frac{1}{2^{(i+j)}} n_{d,i}^* n_{d,j} \alpha_i^{(1)*} \alpha_j^{(2)} \sum_{p=0}^i \sum_{q=0}^j (-1)^q \binom{i}{p} \binom{j}{q} \\
&\quad \times \cos\left(\frac{\pi(p+q)}{2}\right) \frac{(p+q)!}{(p+q)/2)!} \frac{(i+j-p-q)!}{(i+j-p-q)/2)!}. \tag{53}
\end{aligned}$$

The same expression can also be calculated from the general multi-mode kernel (Eq. (46), by setting $m = 1$, $n = d - 1$ and $\beta_j = n_{d,j} \alpha_j$ (see appendix G.1), showing that *all* quantum kernels that can be written as Eq. (8) can be written as either an algebraic function, a Gaussian, or the product of a Gaussian and an algebraic function.

7 Conclusions & future work

In this paper we use the holomorphic representation of continuous variable quantum states to mathematically describe how one might encode data for CV quantum kernel machine learning. In doing so, we are able to identify that all quantum kernels of finite stellar rank can be expressed analytically as products of Gaussian and algebraic function terms. In the case where the algebraic function reduces to a polynomial, the measure of stellar rank, a quantity that is easy to characterise for practical bosonic implementations, neatly captures the classical hardness of simulating these kernels, which scales as $\mathcal{O}(2^{4n})$. We then prove kernels defined by feature maps of infinite stellar rank, such as GKP-state encodings, can be approximated arbitrarily well by kernels defined by feature maps of finite stellar rank. Furthermore, by analysing two simple CV kernels which are expressed as the product of a Gaussian and a polynomial, we are able to develop intuition for how such kernels will behave as we increase their “quantumness” as measured by stellar rank. We see that it is likely that one will encounter problems analogous to exponential concentration, and while bandwidth tuning may mitigate this to some extent, this will trade-off with maintaining effective stellar rank and robustness to shot noise. We have also shown that it is possible to construct characteristic CV quantum kernels that embody both translational and rotational invariance, with an explicit example given as a kernel constructed by a displaced Fock state. We leverage this structure, by creating a supervised learning classification task on annular data. We find that displaced Fock state kernel is well suited for this task, and the classification accuracy increases with increasing stellar rank.

We have also shown that while multi-mode CV quantum kernels are more complex, they can nonetheless still always be expressed as a product of Gaussian and algebraic function terms. Although the notion of stellar rank can no longer be used quantify the classical hardness of direct simulation of these kernel functions, except for a subclass where the algebraic function reduces to a polynomial, the difficulty of simulating the feature maps still scales as $\mathcal{O}(2^n)$. Additionally, since the form of the algebraic function component contains two polynomials, we would not expect simulation to be less complex a single polynomial. While we haven’t simulated such kernels here, we would expect similar behaviour in terms of kernel value suppression beyond a threshold value due to the Gaussian term, and also increasing stellar rank.

It will be important in future work to quantitatively characterise the bandwidth generated trade-offs for particular target problems and specific physical implementations. We also leave for future work an analysis to consider the effects of various appropriate noise models.

Acknowledgements

This work has been supported by the Australian Research Council (ARC) by Centre of Excellence for Engineered Quantum Systems (EQUS, CE170100009). We wish to thank Aleesha Isaacs, Carolyn Wood, Riddhi Gupta, Gerard Milburn, Andrew White and Nicolas Menicucci for useful discussions.

References

- [1] Maria Schuld and Francesco Petruccione. “Quantum models as kernel methods”. [Pages 217–245](#). Springer International Publishing. Cham (2021).
- [2] Maria Schuld and Nathan Killoran. “Quantum machine learning in feature Hilbert spaces”. [Phys. Rev. Lett. **122**, 040504](#) (2019).
- [3] Peter Wittek. “Quantum machine learning: What quantum computing means to data mining”. [Academic Press is an imprint of Elsevier](#). (2016).
- [4] Ian Goodfellow, Yoshua Bengio, and Aaron Courville. “Deep learning”. MIT Press. (2016). url: <http://www.deeplearningbook.org>.
- [5] Yao-Hung Hubert Tsai, Shaojie Bai, Makoto Yamada, Louis-Philippe Morency, and Ruslan Salakhutdinov. “Transformer dissection: An unified understanding for transformer’s attention via the lens of kernel”. In Kentaro Inui, Jing Jiang, Vincent Ng, and Xiaojun Wan, editors, Proceedings of the 2019 Conference on Empirical Methods in Natural Language Processing and the 9th International Joint Conference on Natural Language Processing (EMNLP-IJCNLP). [Pages 4344–4353](#). Hong Kong, China (2019). Association for Computational Linguistics.
- [6] Mikołaj Bińkowski, Dougal J. Sutherland, Michael Arbel, and Arthur Gretton. “Demystifying MMD GANs”. In International Conference on Learning Representations. (2018). url: <https://openreview.net/forum?id=r1lU0zWCW>.
- [7] Jovana Mitrovic, Dino Sejdinovic, and Yee Whye Teh. “Causal inference via kernel deviance measures”. [Advances in neural information processing systems](#)**31** (2018).
- [8] Senjian An, Wanquan Liu, and Svetha Venkatesh. “Face recognition using kernel ridge regression”. In 2007 IEEE Conference on Computer Vision and Pattern Recognition. [Pages 1–7](#). (2007).
- [9] Weifeng Liu, Il Park, and José C. Principe. “An information theoretic approach of designing sparse kernel adaptive filters”. [IEEE Transactions on Neural Networks](#) **20**, 1950–1961 (2009).
- [10] Shotaro Akaho. “A kernel method for canonical correlation analysis” (2007). [arXiv:cs/0609071](https://arxiv.org/abs/cs/0609071).
- [11] Mikhail Belkin, Siyuan Ma, and Soumik Mandal. “To understand deep learning we need to understand kernel learning”. In Jennifer Dy and Andreas Krause, editors, Proceedings of the 35th International Conference on Machine Learning. Volume 80 of Proceedings of Machine Learning Research, pages 541–549. PMLR (2018). url: <https://proceedings.mlr.press/v80/belkin18a.html>.

- [12] Youngmin Cho and Lawrence Saul. “Kernel methods for deep learning”. In Y. Bengio, D. Schuurmans, J. Lafferty, C. Williams, and A. Culotta, editors, *Advances in Neural Information Processing Systems*. Volume 22. Curran Associates, Inc. (2009). url: https://proceedings.neurips.cc/paper_files/paper/2009/file/5751ec3e9a4feab575962e78e006250d-Paper.pdf.
- [13] Thomas Hubregtsen, David Wierichs, Elies Gil-Fuster, Peter-Jan H. S. Derks, Paul K. Faehrmann, and Johannes Jakob Meyer. “Training quantum embedding kernels on near-term quantum computers”. *Physical Review A* **106** (2022).
- [14] Casper Gyurik, van Dyon Vreumingen, and Vedran Dunjko. “Structural risk minimization for quantum linear classifiers”. *Quantum* **7**, 893 (2023).
- [15] Sofiene Jerbi, Lukas J. Fiderer, Hendrik Poulsen Nautrup, Jonas M. Kübler, Hans J. Briegel, and Vedran Dunjko. “Quantum machine learning beyond kernel methods”. *Nature Communications* **14** (2023).
- [16] Yunchao Liu, Srinivasan Arunachalam, and Kristan Temme. “A rigorous and robust quantum speed-up in supervised machine learning”. *Nature Physics* **17**, 1013–1017 (2021).
- [17] Jennifer R. Glick, Tanvi P. Gujarati, Antonio D. Corcoles, Youngseok Kim, Abhinav Kandala, Jay M. Gambetta, and Kristan Temme. “Covariant quantum kernels for data with group structure” (2022). [arXiv:2105.03406](https://arxiv.org/abs/2105.03406).
- [18] Vojtěch Havlíček, Antonio D. Córcoles, Kristan Temme, Aram W. Harrow, Abhinav Kandala, Jerry M. Chow, and Jay M. Gambetta. “Supervised learning with quantum-enhanced feature spaces”. *Nature* **567**, 209–212 (2019).
- [19] Hsin-Yuan Huang, Michael Broughton, Jordan Cotler, Sitan Chen, Jerry Li, Masoud Mohseni, Hartmut Neven, Ryan Babbush, Richard Kueng, John Preskill, and Jarrod R. McClean. “Quantum advantage in learning from experiments”. *Science* **376**, 1182–1186 (2022). [arXiv:https://www.science.org/doi/pdf/10.1126/science.abn7293](https://arxiv.org/abs/https://www.science.org/doi/pdf/10.1126/science.abn7293).
- [20] Jarrod R. McClean, Sergio Boixo, Vadim N. Smelyanskiy, Ryan Babbush, and Hartmut Neven. “Barren plateaus in quantum neural network training landscapes”. *Nature Communications* **9** (2018).
- [21] Supanut Thanasilp, Samson Wang, M. Cerezo, and Zoë Holmes. “Exponential concentration and untrainability in quantum kernel methods” (2022). [arXiv:2208.11060](https://arxiv.org/abs/2208.11060).
- [22] Jonas M. Kübler, Simon Buchholz, and Bernhard Scholkopf. “The inductive bias of quantum kernels”. In *Neural Information Processing Systems*. (2021). url: <https://api.semanticscholar.org/CorpusID:235358860>.
- [23] Hsin-Yuan Huang, Michael Broughton, Masoud Mohseni, Ryan Babbush, Sergio Boixo, Hartmut Neven, and Jarrod R. McClean. “Power of data in quantum machine learning”. *Nature Communications* **12** (2021).
- [24] Abdulkadir Canatar, Evan Peters, Cengiz Pehlevan, Stefan M. Wild, and Ruslan Shaydulin. “Bandwidth enables generalization in quantum kernel models”. *Transactions on Machine Learning Research* (2023). url: <https://openreview.net/forum?id=A1N2qp4yAq>.
- [25] Abdulkadir Canatar. “Statistical mechanics of generalization in kernel regression and wide neural networks”. Doctoral dissertation. Harvard University Graduate School of Arts and Sciences. (2022).
- [26] Bernhard Schölkopf and Alexander J. Smola. “Learning with kernels: Support vector machines, regularization, optimization and beyond”. *MIT press*. (2002).
- [27] Lucas Slattey, Ruslan Shaydulin, Shouvanik Chakrabarti, Marco Pistoia, Sami Khairy, and Stefan M. Wild. “Numerical evidence against advantage with quantum fidelity kernels on classical data”. *Physical Review A* **107** (2023).

- [28] Michael Ragone, Paolo Braccia, Quynh T. Nguyen, Louis Schatzki, Patrick J. Coles, Frederic Sauvage, Martin Larocca, and M. Cerezo. “Representation theory for geometric quantum machine learning” (2023). [arXiv:2210.07980](#).
- [29] Roohollah Ghobadi. “Nonclassical kernels in continuous-variable systems”. *Phys. Rev. A* **104**, 052403 (2021).
- [30] Prayag Tiwari, Shahram Dehdashti, Abdul Karim Obeid, Pekka Marttinen, and Peter Bruza. “Kernel method based on non-linear coherent states in quantum feature space”. *Journal of Physics A: Mathematical and Theoretical* **55**, 355301 (2022).
- [31] Junyu Liu, Changchun Zhong, Matthew Otten, Anirban Chandra, Cristian L Cortes, Chaoyang Ti, Stephen K Gray, and Xu Han. “Quantum Kerr learning”. *Machine Learning: Science and Technology* **4**, 025003 (2023).
- [32] C Bowie, S Shrapnel, and M J Kewming. “Quantum kernel evaluation via Hong–Ou–Mandel interference”. *Quantum Science and Technology* **9**, 015001 (2023).
- [33] Ulysse Chabaud and Saeed Mehraban. “Holomorphic representation of quantum computations”. *Quantum* **6**, 831 (2022).
- [34] Ulysse Chabaud and Mattia Walschaers. “Resources for bosonic quantum computational advantage”. *Physical Review Letters* **130** (2023).
- [35] Thomas Hofmann, Bernhard Schölkopf, and Alexander J. Smola. “Kernel methods in machine learning”. *The Annals of Statistics* **36** (2008).
- [36] Bernhard Schölkopf, Ralf Herbrich, and Alex J. Smola. “A generalized representer theorem”. *Lecture Notes in Computer Science* **Page 416–426** (2001).
- [37] Bharath K. Sriperumbudur, Kenji Fukumizu, and Gert R.G. Lanckriet. “Universality, characteristic kernels and RKHS embedding of measures”. *Journal of Machine Learning Research* **12**, 2389–2410 (2011). url: <http://jmlr.org/papers/v12/sriperumbudur11a.html>.
- [38] John Shawe-Taylor and Nello Cristianini. “Kernel methods for pattern analysis”. *Cambridge University Press*. (2004).
- [39] Vladimir V’yugin. “VC dimension, fat-shattering dimension, Rademacher averages, and their applications”. *Measures of Complexity: Festschrift for Alexey Chervonenkis* **Pages 57–74** (2015).
- [40] Oskar Allerbo and Rebecka Jörnsten. “Bandwidth selection for Gaussian kernel ridge regression via Jacobian control” (2023). [arXiv:2205.11956](#).
- [41] D Gottesman. “The Heisenberg representation of quantum computers”. *U.S. Department of Energy Office of Scientific and Technical Information* (1998).
- [42] Stephen D. Bartlett, Barry C. Sanders, Samuel L. Braunstein, and Kae Nemoto. “Efficient classical simulation of continuous variable quantum information processes”. *Phys. Rev. Lett.* **88**, 097904 (2002).
- [43] Gottesman A. Kitaev and J. Preskill. “Encoding a qubit in an oscillator”. *Physical Review A* **64**, 012310 (2001).
- [44] U. Chabaud, M. Walschaers G. Roeland, F. Grosshans, D. Markham V. Parigi, and N. Trep. “Certification of non-Gaussian states with operational measurements”. *PRX Quantum* **2** (2021).
- [45] BK. Sriperumbudur, A. Gretton, K. Fukumizu, G. Lanckriet, and B. Schölkopf. “Injective Hilbert space embeddings of probability measures”. In *Proceedings of the 21st Annual Conference on Learning Theory*. **Pages 111–122**. Madison, WI, USA (2008). Max-Planck-Gesellschaft. Omnipress.
- [46] Clayton Scott and Kristjan Greenewald. “Universal consistency of SVMs and other kernel methods” (2014).

- [47] V. Bargmann. “On a Hilbert space of analytic functions and an associated integral transform part I”. [Communications on Pure and Applied Mathematics](#) **14**, 187–214 (1961).
- [48] Vern I. Paulsen and Mrinal Raghupathi. “An introduction to the theory of reproducing kernel Hilbert spaces”. [Cambridge Studies in Advanced Mathematics](#). Cambridge University Press. (2016).
- [49] “*NIST Digital Library of Mathematical Functions*”. <https://dlmf.nist.gov/>, Release 1.1.11 of 2023-09-15. F. W. J. Olver, A. B. Olde Daalhuis, D. W. Lozier, B. I. Schneider, R. F. Boisvert, C. W. Clark, B. R. Miller, B. V. Saunders, H. S. Cohl, and M. A. McClain, eds.
- [50] Eric W. Weisstein. “Binomial coefficient”. url: <https://mathworld.wolfram.com/BinomialCoefficient.html>. Visited on 05/01/24.

Supplementary Material

A Proof that inner products are positive semi-definite

Remark 1. *Inner Products of the form $\langle \cdot | \cdot \rangle : \mathcal{H} \times \mathcal{H} \rightarrow \mathbb{C}$ are positive semi-definite.*

A matrix \mathbf{M} is positive semi-definite if and only if

$$\mathbf{x}^\dagger \mathbf{M} \mathbf{x} \geq 0 \quad \forall \mathbf{x} \in \mathbb{C}^n. \quad (54)$$

We can construct our Gram Matrix, \mathbf{G} , from our defined inner product by

$$G_{i,j} = \langle \mathbf{v}_i | \mathbf{v}_j \rangle, \quad (55)$$

for $\mathbf{v}_i, \mathbf{v}_j \in \mathcal{H}$.

Hence to show the inner product is positive semi-definite, it is sufficient to show the gram matrix is positive semi-definite. We can see for any $\mathbf{x} \in \mathbb{C}^n$,

$$\mathbf{x}^\dagger \mathbf{G} \mathbf{x} = \sum_{i,j} x_i^* G_{i,j} x_j \quad (56)$$

$$= \sum_{i,j} x_i^* \langle \mathbf{v}_i | \mathbf{v}_j \rangle x_j \quad (57)$$

$$= \sum_{i,j} \langle x_i^* \mathbf{v}_i | x_j \mathbf{v}_j \rangle \quad (58)$$

$$= \left\langle \sum_i x_i^* \mathbf{v}_i \left| \sum_j x_j \mathbf{v}_j \right. \right\rangle \quad (59)$$

$$= \left\| \sum_i x_i^* \mathbf{v}_i \right\|^2 \geq 0 \quad (60)$$

Remark 2. *Note that by definition, inner products are also conjugate symmetric. That is,*

$$\langle x | y \rangle = \langle y | x \rangle^*. \quad (61)$$

B Properties of Segal-Bargmann Space

Here we present 2 interesting properties of the Segal-Bargmann space, firstly that it is a RKHS of the Gaussian kernel, and secondly that unitaries applied to holomorphic functions, remain as a holomorphic function.

B.1 Segal-Bargmann space is a RKHS of the Gaussian kernel

Our formulation of CV quantum kernels heavily utilises the Segal-Bargmann space. Knowing properties about this space can allow us to further develop our kernels. Here we explicitly prove that this space contains the Gaussian kernel which is well known to be universal. We can also show that this kernel is universal. Universality of kernels is a measure of their expressibility, characterising how well the kernel can classify the data from a metric space. A universal kernel is one which can learn any function for empirical loss minimisation from

equation 2. To prove such a property we can show that the RKHS is dense inside the space of continuous functions ($\mathcal{C}(\mathcal{X})$) of our data. This is equivalent to showing that the kernel, decomposed into a power series of inner products, has only positive coefficients [46].

The following proof is adapted from [47]. Let us denote our reproducing kernel as $\mathbf{e}_a \in \mathcal{H}_{SB}$ for some fixed $a \in \mathcal{C}^n$. Hence by properties of the evaluation functional we have,

$$f(a) = \langle \mathbf{e}_a | f \rangle. \quad (62)$$

By the definition of the inner product in the SB space we can rewrite this as,

$$f(a) = \int_{\mathcal{C}^m} d^{2m}z \, \mathbf{e}_a^*(z) f(z). \quad (63)$$

Here we can see that the reproducing kernel $\mathbf{e}_a^*(z) = \mathcal{K}(a, z)$ is the kernel function for the SB space. By definition (equation 62) we have,

$$\mathbf{e}_a(z) = \langle \mathbf{e}_z | \mathbf{e}_a \rangle, \quad (64)$$

and so we yield,

$$\mathcal{K}(a, z) = \langle \mathbf{e}_a | \mathbf{e}_z \rangle. \quad (65)$$

In terms of any complete orthonormal set, v_h we can write the evaluational functional as,

$$\mathbf{e}_a = \lim_{k \rightarrow \infty} \sum_{h=1}^k \langle v_h | \mathbf{e}_a \rangle v_h = \lim_{k \rightarrow \infty} \sum_{h=1}^k v_h^*(a) v_h. \quad (66)$$

We know that strong convergence (a proven property of the SB space) implies pointwise converge which yields,

$$\mathbf{e}_a(z) = \sum_h v_h^*(a) v_h(z), \quad (67)$$

regardless of which orthonormal basis v_h we choose. If we specify a specific basis, namely,

$$u_{[m]}(z) = \prod_k \frac{z_k^{m_k}}{\sqrt{m_k!}}, \quad (68)$$

where m_k is a monotone increasing sequence of integers, we find,

$$\mathbf{e}_a(z) = \sum_m \prod_k \frac{(a_k^* z_k)^{m_k}}{m_k!} = e^{a^* \cdot z}, \quad (69)$$

as the gaussian reproducing kernel. It is well known that the gaussian kernel, expanded into a power series in the inner product of our data space, has positive coefficients. As such, the SB space is an RKHS with a universal kernel. This is useful as gaussian kernels are the foundation of classical machine learning and through the SB space, our quantum kernel has direct access to this kernel [47, 48].

B.2 Unitary evolutions of quantum states mapped to holomorphic functions are also holomorphic functions.

We can recall that a unitary evolution is generated by a Hamiltonian which is a self-adjoint function of the creation and annihilation operators such that,

$$\hat{U} = e^{-i\hat{H}(\hat{a}, \hat{a}^\dagger)t} = \sum_{j=0}^{\infty} \frac{(-it)^j}{j!} \left(\hat{H}(\hat{a}, \hat{a}^\dagger) \right)^j. \quad (70)$$

The Hamiltonian can also be written as a self-adjoint complex power series in \hat{a} and \hat{a}^\dagger ,

$$\hat{H}(\hat{a}, \hat{a}^\dagger) = \sum_k \sum_{\hat{A} \in \{\hat{a}, \hat{a}^\dagger\}^k} \alpha_{k, \hat{A}} \hat{A}, \quad (71)$$

where $\alpha_{k, \hat{A}} \in \mathbb{C}$ (such that \hat{H} is self-adjoint) and $\{\hat{a}, \hat{a}^\dagger\}^k$ is the set (with length 2^k) of multiplicative permutations of creation and annihilation operators with length k .

Substituting the Hamiltonian equation (71) into the unitary equation we can write any unitary operation applied to an initial state $|\psi\rangle$ as,

$$\hat{U} |\psi\rangle = \sum_{j=0}^{\infty} \frac{(-it)^j}{j!} \left(\sum_k \sum_{\sigma \in \{\hat{a}, \hat{a}^\dagger\}^k} \alpha_{k, \hat{A}} \hat{A} \right)^j |\psi\rangle. \quad (72)$$

Overall, this yields a sum of terms, each of which are a multiplication of creation and annihilation operators applied to $|\psi\rangle$.

If we convert to holomorphic functions as in section 3 ($|\psi\rangle \mapsto F_\psi^*(z)$), we see the annihilation and creation operators are transformed to differential operators. Hence to show the unitaries preserve holomorphic functions, we can show that sums of products of differential operators $z \times$ and ∂_z keep the holomorphic function in SB space.

Firstly let us see that annihilation and creation operators individually keeps a holomorphic function in SB space.

We recall that quantum states can be mapped to holomorphic functions and those with finite stellar rank can be written as shown in equation 14.

If we apply $(z \times)$ to such a state we yield,

$$z \left(e^{-a/2z^2+bz+c} \sum_{j=0}^n \beta_j z^j \right) = e^{-a/2z^2+bz+c} \sum_{j=0}^n \beta_j z^{j+1}, \quad (73)$$

which remains in the form $G(z)P(z)$ as a stellar function of rank $n+1$.

If we apply the operator ∂_z to the state we find,

$$\partial_z \left(e^{-a/2z^2+bz+c} \sum_{j=0}^n \beta_j z^j \right) = e^{-a/2z^2+bz+c} \left[(-az+b) \left(\sum_{j=0}^n \beta_j z^j \right) + \left(\sum_{j=0}^n j \beta_j z^{j-1} \right) \right], \quad (74)$$

which can be easily factored into the form $G(z)P(z)$ as,

$$= e^{-a/2z^2+bz+c} \left(\sum_{j=0}^n -a \beta_j z^{j+1} + b \beta_j z^j + j \beta_j z^{j-1} \right) \quad (75)$$

hence remaining as a stellar function.

As each operation keeps our stellar function in the SB space, it follows that repeated operations also preserve the functions in SB space.

We note that neither of the operations change the Gaussian part of the stellar function, only the polynomial term is changed.

Now we consider sums of products of operators. Let us consider an operator,

$$\sum_k \alpha_k \hat{A}_k, \quad (76)$$

where $\alpha_k \in \mathbb{C}$ and \hat{A}_k is a product of the operators $z \times$ and ∂_z . As the Hilbert space of holomorphic functions (the SB space) is complete, any summation of elements in the space remains in the space. Hence the summation of products of operators clearly keeps a Holomorphic function in the SB space.

Hence any unitary operation - which are constructed by sums of products of operators - applied to a quantum state mapped to holomorphic functions in SB space, remain in SB space.

Finally, it is interesting to note that any unitary operation does not change the Gaussian term of stellar functions, instead only changing the polynomial term - hence often changing the rank of the stellar function.

C An integration required to calculate the closed form of CV kernels

In this section we will calculate the integral

$$I_n(a, b) := \int_{-\infty}^{\infty} dx \exp(-ax^2 + bx) x^n \quad (77)$$

for $a, b \in \mathbb{C}$ with $\text{Re}(a) > 0$ and $n \in \mathbb{N}_0$. Since CV quantum states, when represented as holomorphic functions, are always a product of a Gaussian and a polynomial, the evaluation of any CV quantum kernel will require the evaluation of integrals of the form of Eq. (77).

C.1 Explicit calculation

The explicit evaluation of Eq. (77) is

$$\begin{aligned} I_n(a, b) &:= \int_{-\infty}^{\infty} dx \exp(-ax^2 + bx) x^n \\ &= a^{-(n+1)/2} \left[\frac{1 + (-1)^n}{2} \Gamma\left(\frac{1}{2} + \frac{n}{2}\right) {}_1F_1\left(\frac{1}{2} + \frac{n}{2}; \frac{1}{2}; \frac{b^2}{4a}\right) \right. \\ &\quad \left. + \frac{1 + (-1)^{n+1}}{2} \Gamma\left(\frac{3}{2} + \frac{n-1}{2}\right) \frac{b}{\sqrt{a}} {}_1F_1\left(\frac{3}{2} + \frac{n-1}{2}; \frac{3}{2}; \frac{b^2}{4a}\right) \right] \end{aligned} \quad (78)$$

where ${}_1F_1$ is the confluent hypergeometric function, which have the property that for $n \in \mathbb{N}_0$:

$${}_1F_1(b + n; b; \zeta) = e^\zeta \sum_{j=0}^n \binom{n}{j} \frac{\zeta^j}{(b)_j} \quad (79)$$

where $(b)_j$ is the Pochhammer symbol

$$(b)_j := \frac{\Gamma(b + j)}{\Gamma(b)}.$$

We explicitly prove Eq. (79) in section C.2.

By considering the cases of even n and odd n separately, Eq. (79) can be used to simply Eq. (78) and write it as a product of a Gaussian and a polynomial.

When n is even:

$$\begin{aligned}
I_n(a, b) &= a^{-(n+1)/2} \Gamma\left(\frac{1}{2} + \frac{n}{2}\right) {}_1F_1\left(\frac{1}{2} + \frac{n}{2}; \frac{1}{2}; \frac{b^2}{4a}\right) \\
&= a^{-(n+1)/2} \Gamma\left(\frac{1}{2} + \frac{n}{2}\right) \exp\left(\frac{b^2}{4a}\right) \sum_{j=0}^{n/2} \binom{n/2}{j} \frac{1}{2^{2j}(1/2)_j} \left(\frac{b}{\sqrt{a}}\right)^{2j} \\
&= a^{-(n+1)/2} \exp\left(\frac{b^2}{4a}\right) \sum_{k=0}^n \gamma_{n,k}^{(\text{even})} \left(\frac{b}{\sqrt{a}}\right)^k
\end{aligned} \tag{80}$$

where

$$\gamma_{n,k}^{(\text{even})} := \begin{cases} \Gamma\left(\frac{1}{2} + \frac{n}{2}\right) \binom{n/2}{k/2} \frac{1}{2^{k(1/2)_{k/2}}}, & k \text{ even} \\ 0, & k \text{ odd} \end{cases} \tag{81}$$

and when n is odd:

$$\begin{aligned}
I_n(a, b) &= a^{-(n+1)/2} \Gamma\left(\frac{3}{2} + \frac{n-1}{2}\right) \frac{b}{\sqrt{a}} {}_1F_1\left(\frac{3}{2} + \frac{n-1}{2}; \frac{3}{2}; \frac{b^2}{4a}\right) \\
&= a^{-(n+1)/2} \Gamma\left(\frac{3}{2} + \frac{n-1}{2}\right) \exp\left(\frac{b^2}{4a}\right) \sum_{j=0}^{(n-1)/2} \binom{(n-1)/2}{j} \frac{1}{2^{2j}(3/2)_j} \left(\frac{b}{\sqrt{a}}\right)^{2j+1} \\
&= a^{-(n+1)/2} \exp\left(\frac{b^2}{4a}\right) \sum_{k=0}^n \gamma_{n,k}^{(\text{odd})} \left(\frac{b}{\sqrt{a}}\right)^k
\end{aligned} \tag{82}$$

where

$$\gamma_{n,k}^{(\text{odd})} := \begin{cases} \Gamma\left(\frac{3}{2} + \frac{n-1}{2}\right) \binom{(n-1)/2}{(k-1)/2} \frac{1}{2^{k-1}(3/2)_{(k-1)/2}}, & k \text{ odd} \\ 0, & k \text{ even.} \end{cases} \tag{83}$$

Therefore, combining Eqns. (82) and (80) gives the general result:

$$I_n(a, b) = a^{-(n+1)/2} \exp\left(\frac{b^2}{4a}\right) \sum_{j=0}^n \gamma_{n,j} \left(\frac{b}{\sqrt{a}}\right)^j \tag{84}$$

where

$$\gamma_{n,j} := \begin{cases} \Gamma\left(\frac{1}{2} + \frac{n}{2}\right) \binom{n/2}{j/2} \frac{1}{2^{j(1/2)_{j/2}}}, & n, j \text{ even} \\ \Gamma\left(\frac{3}{2} + \frac{n-1}{2}\right) \binom{(n-1)/2}{(j-1)/2} \frac{1}{2^{j-1}(3/2)_{(j-1)/2}}, & n, j \text{ odd} \\ 0, & \text{otherwise.} \end{cases} \tag{85}$$

C.2 Proof the confluent hypergeometric function $({}_1F_1(b+n; b; \zeta))$ is a product of an exponential and a polynomial

In this section, we explicitly prove Eq. (79) and show a confluent hypergeometric function of the form ${}_1F_1(b+n; b; \zeta)$ can be written as a product of an exponential and a polynomial of degree n .

This proof requires two properties of confluent hypergeometric functions[49, (13.6.1),(13.3.4)]

$${}_1F_1(b; b; \zeta) = e^\zeta \quad (86a)$$

$${}_1F_1(a; b; \zeta) = {}_1F_1(a-1; b; \zeta) + \frac{\zeta}{b} {}_1F_1(a; b+1; \zeta). \quad (86b)$$

Proposition: For $n \in \mathbb{N}_0$, the confluent hypergeometric function

$${}_1F_1(b+n; b; \zeta) = e^\zeta \sum_{j=0}^n \binom{n}{j} \frac{\zeta^j}{(b)_j} \quad (87)$$

where $(b)_j$ is the Pochhammer symbol.

Proof (by induction):

The base case for $n = 0$ is given in Eq. (86a).

Assume that Eq. (87) holds for n and consider the $n+1$ case

$$\begin{aligned} {}_1F_1(b+n+1; b; \zeta) &= {}_1F_1(b+n; b; \zeta) + \frac{\zeta}{b} {}_1F_1(b+n+1; b+1; \zeta) \\ &= e^\zeta \sum_{j=0}^n \binom{n}{j} \frac{\zeta^j}{(b)_j} + \frac{\zeta}{b} \left(e^\zeta \sum_{j=0}^n \binom{n}{j} \frac{\zeta^j}{(b+1)_j} \right) \\ &= e^\zeta \left(\sum_{j=0}^n \binom{n}{j} \frac{\zeta^j}{(b)_j} + \sum_{j=0}^n \binom{n}{j} \frac{\Gamma(b+1)}{\Gamma(b+j+1)} \frac{\zeta^{j+1}}{b} \right) \\ &= e^\zeta \left(\sum_{j=0}^n \binom{n}{j} \frac{\zeta^j}{(b)_j} + \sum_{k=1}^{n+1} \binom{n}{k-1} \frac{\Gamma(b)}{\Gamma(b+k)} \zeta^k \right) \\ &= e^\zeta \left(1 + \sum_{j=1}^n \binom{n}{j} \frac{\zeta^j}{(b)_j} + \sum_{j=1}^n \binom{n}{j-1} \frac{\zeta^j}{(b)_j} + \frac{\zeta^{n+1}}{(b)_n} \right) \\ &= e^\zeta \left(1 + \sum_{j=1}^n \binom{n+1}{j} \frac{\zeta^j}{(b)_j} + \frac{\zeta^{n+1}}{(b)_n} \right) \quad (\text{Pascal's identity}) \\ &= e^\zeta \sum_{j=0}^{n+1} \binom{n+1}{j} \frac{\zeta^j}{(b)_j}. \end{aligned} \quad (88)$$

Therefore if Eq. (87) holds for n then it holds for $n+1$.

By the induction rule, Eq. (87) holds for all $n \in \mathbb{N}_0$. \square

D Properties of the displaced Fock state kernel

In this section we show the details of the derivation and properties of the displaced Fock state kernel (Eq. (26)).

D.1 Derivation of Eq. (26)

The displaced Fock state inner product is calculated from Eq. (25) by first setting $z = x+iy$ and applying the trinomial expansion so that the x and y integrals can be written in the form of Eq. (84).

$$\begin{aligned}
\langle F_\alpha^*(z) | F_\beta^*(z) \rangle &= \frac{1}{\pi} \frac{e^{-(|\alpha|^2+|\beta|^2)/2}}{n!} \int_{-\infty}^{\infty} dx \int_{-\infty}^{\infty} dy e^{-(x^2+y^2)+\alpha^*(x-iy)+\beta(x+iy)} \\
&\quad \times (x-iy-\alpha)^n (x+iy-\beta^*)^n \\
&= \frac{1}{\pi} \frac{e^{-(|\alpha|^2+|\beta|^2)/2}}{n!} \int_{-\infty}^{\infty} dx \int_{-\infty}^{\infty} dy e^{-x^2+(\alpha^*+\beta)x} e^{-y^2-i(\alpha^*-\beta)y} \\
&\quad \times \left(\sum_{i=0}^n \sum_{j=0}^{n-i} \frac{n!}{i!j!(n-i-j)!} x^i (-iy)^j (-\alpha)^{n-i-j} \right) \\
&\quad \times \left(\sum_{k=0}^n \sum_{\ell=0}^{n-k} \frac{n!}{k!\ell!(n-k-\ell)!} x^k (iy)^\ell (-\beta^*)^{n-k-\ell} \right) \\
&= \frac{n!}{\pi} e^{-(|\alpha|^2+|\beta|^2)/2} \sum_{i=0}^n \sum_{j=0}^{n-i} \sum_{k=0}^n \sum_{\ell=0}^{n-k} \frac{(-i)^j (-\alpha)^{n-i-j}}{i!j!(n-i-j)!} \frac{(i)^\ell (-\beta^*)^{n-k-\ell}}{k!\ell!(n-k-\ell)!} \\
&\quad \times \left(\int_{-\infty}^{\infty} dx e^{-x^2+(\alpha^*+\beta)x} x^{i+k} \right) \left(\int_{-\infty}^{\infty} dy e^{-y^2-i(\alpha^*-\beta)y} y^{j+\ell} \right) \\
&= \frac{n!}{\pi} e^{-(|\alpha|^2+|\beta|^2)/2} \sum_{i=0}^n \sum_{j=0}^{n-i} \sum_{k=0}^n \sum_{\ell=0}^{n-k} \frac{(-i)^j (-\alpha)^{n-i-j}}{i!j!(n-i-j)!} \frac{(i)^\ell (-\beta^*)^{n-k-\ell}}{k!\ell!(n-k-\ell)!} \\
&\quad \times I_{i+k}(1, (\alpha^*+\beta)) I_{j+\ell}(1, -i(\alpha^*-\beta)) \tag{89}
\end{aligned}$$

Now using Eq. (84), the displacement inner product can be directly written as:

$$\begin{aligned}
\langle F_\alpha^*(z) | F_\beta^*(z) \rangle &= \frac{n!}{\pi} e^{-(|\alpha|^2+|\beta|^2)/2} e^{\alpha^*\beta} \sum_{i=0}^n \sum_{j=0}^{n-i} \sum_{k=0}^n \sum_{\ell=0}^{n-k} \sum_{p=0}^{i+k} \sum_{q=0}^{j+\ell} \frac{(-i)^j (-\alpha)^{n-i-j}}{i!j!(n-i-j)!} \\
&\quad \times \frac{(i)^\ell (-\beta^*)^{n-k-\ell}}{k!\ell!(n-k-\ell)!} \gamma_{(i+k),p} \gamma_{(j+\ell),q} (\alpha^*+\beta)^p (-i(\alpha^*-\beta))^q \tag{90}
\end{aligned}$$

which is the product of a Gaussian and a polynomial of degree $2n$ in α and β .

D.2 Explicit examples of the displaced Fock state kernel

In this section we write down the explicit form of the first nine displacement kernels.

Initial Fock state, $ n\rangle$	Kernel function, $k(\alpha, \beta)$
$ 0\rangle$	$e^{- \alpha-\beta ^2}$
$ 1\rangle$	$e^{- \alpha-\beta ^2} (\alpha-\beta ^2 - 1)^2$
$ 2\rangle$	$\frac{e^{- \alpha-\beta ^2}}{4} (2 - 4 \alpha-\beta ^2 + \alpha-\beta ^4)^2$
$ 3\rangle$	$\frac{e^{- \alpha-\beta ^2}}{36} (-6 + 18 \alpha-\beta ^2 - 9 \alpha-\beta ^4 + \alpha-\beta ^6)^2$
$ 4\rangle$	$\frac{e^{- \alpha-\beta ^2}}{576} (24 - 96 \alpha-\beta ^2 + 72 \alpha-\beta ^4 - 16 \alpha-\beta ^6 + \alpha-\beta ^8)^2$
$ 5\rangle$	$\frac{e^{- \alpha-\beta ^2}}{14400} (-120 + 600 \alpha-\beta ^2 - 600 \alpha-\beta ^4 + 200 \alpha-\beta ^6 - 25 \alpha-\beta ^8 + \alpha-\beta ^{10})^2$
$ 6\rangle$	$\frac{e^{- \alpha-\beta ^2}}{518400} (720 - 4320 \alpha-\beta ^2 + 5400 \alpha-\beta ^4 - 2400 \alpha-\beta ^6 + 450 \alpha-\beta ^8 - 36 \alpha-\beta ^{10} + \alpha-\beta ^{12})^2$
$ 7\rangle$	$\frac{e^{- \alpha-\beta ^2}}{25401600} (-5040 + 35280 \alpha-\beta ^2 - 52920 \alpha-\beta ^4 + 29400 \alpha-\beta ^6 - 7350 \alpha-\beta ^8 + 882 \alpha-\beta ^{10} - 49 \alpha-\beta ^{12} + \alpha-\beta ^{14})^2$
$ 8\rangle$	$\frac{e^{- \alpha-\beta ^2}}{1625702400} (40320 - 322560 \alpha-\beta ^2 + 564480 \alpha-\beta ^4 - 376320 \alpha-\beta ^6 + 117600 \alpha-\beta ^8 - 18816 \alpha-\beta ^{10} + 1568 \alpha-\beta ^{12} - 64 \alpha-\beta ^{14} + \alpha-\beta ^{16})^2$

D.3 Showing the displaced Fock state kernel is translation invariant

A translation invariant kernel has the property that

$$k(\alpha + \mathbf{h}, \beta + \mathbf{h}) = k(\alpha, \beta). \quad (91)$$

For the case of the displaced Fock state kernel, the vector $\mathbf{h} = (h_1, h_2)^\top \in \mathbb{R}^2$, and we define $h = h_1 + ih_2$. Now the shifted kernel is

$$k(\alpha + \mathbf{h}, \beta + \mathbf{h}) = \left| \langle F_{\alpha+h}^*(z) | F_{\beta+h}^*(z) \rangle \right|^2 \quad (92)$$

where

$$\begin{aligned} & \langle F_{\alpha+h}^*(z) | F_{\beta+h}^*(z) \rangle \\ &= \frac{1}{\pi} \frac{e^{-(|\alpha+h|^2 + |\beta+h|^2)/2}}{n!} \int_{z \in \mathbb{C}} d^2z e^{-[|z|^2 - (\alpha^* + h^*)z^* - (\beta + h)z]} (z^* - \alpha - h)^n (z - \beta^* - h^*)^n. \end{aligned} \quad (93)$$

Change variables $z \rightarrow z + h^*$, so the inner product is now

$$\begin{aligned} \langle F_{\alpha+h}^*(z) | F_{\beta+h}^*(z) \rangle &= \frac{1}{\pi} \frac{e^{-(|\alpha+h|^2 + |\beta+h|^2)/2}}{n!} \int_{z \in \mathbb{C}} d^2z e^{-|z+h^*|^2 + (\alpha^* + h^*)(z^* + h) + (\beta + h)(z + h^*)} \\ &= \frac{1}{\pi} \frac{e^{-(|\alpha|^2 + |\beta|^2)/2} e^{[h(\alpha^* - \beta^*) - h^*(\alpha - \beta)]/2}}{n!} \\ &\quad \times \int_{z \in \mathbb{C}} d^2z e^{-(|z| - \alpha^* z^* - \beta z)} (z^* - \alpha)^n (z - \beta^*)^n \\ &= e^{i \operatorname{Im}[h(\alpha^* - \beta^*)]} \langle F_\alpha^*(z) | F_\beta^*(z) \rangle. \end{aligned} \quad (94)$$

Therefore:

$$\begin{aligned}
k(\boldsymbol{\alpha} + \mathbf{h}, \boldsymbol{\beta} + \mathbf{h}) &= \left| \left\langle F_{\alpha+h}^*(z) \middle| F_{\beta+h}^*(z) \right\rangle \right|^2 \\
&= \left(e^{i \operatorname{Im}[h(\alpha^* - \beta^*)]} \left\langle F_{\alpha}^*(z) \middle| F_{\beta}^*(z) \right\rangle \right) \left(e^{-i \operatorname{Im}[h(\alpha^* - \beta^*)]} \left\langle F_{\alpha}^*(z) \middle| F_{\beta}^*(z) \right\rangle^* \right) \\
&= \left| \left\langle F_{\alpha}^*(z) \middle| F_{\beta}^*(z) \right\rangle \right|^2 \\
&= k(\boldsymbol{\alpha}, \boldsymbol{\beta})
\end{aligned} \tag{95}$$

and the displacement kernel is translation invariant.

D.4 Showing the displaced Fock state kernel is rotation invariant

A rotation invariant kernel has the property that

$$k(\mathcal{R}(\theta)\boldsymbol{\alpha}, \mathcal{R}(\theta)\boldsymbol{\beta}) = k(\boldsymbol{\alpha}, \boldsymbol{\beta}). \tag{96}$$

For the case of the displaced Fock state kernel, the rotation matrix is

$$\mathcal{R}(\theta) = \begin{pmatrix} \cos(\theta) & -\sin(\theta) \\ \sin(\theta) & \cos(\theta) \end{pmatrix}. \tag{97}$$

Under this transformation, the complex number $\alpha \rightarrow e^{i\theta}\alpha$, so the rotated kernel is

$$k(\mathcal{R}(\theta)\boldsymbol{\alpha}, \mathcal{R}(\theta)\boldsymbol{\beta}) = \left| \left\langle F_{\exp(i\theta)\alpha}^*(z) \middle| F_{\exp(i\theta)\beta}^*(z) \right\rangle \right|^2, \tag{98}$$

where

$$\begin{aligned}
\left\langle F_{\exp(i\theta)\alpha}^*(z) \middle| F_{\exp(i\theta)\beta}^*(z) \right\rangle &= \frac{1}{\pi} \frac{e^{-(|\alpha|^2 + |\beta|^2)/2}}{n!} \int_{z \in \mathbb{C}} d^2 z e^{-[|z|^2 - \exp(-i\theta)\alpha^* z^* - \exp(i\theta)\beta z]} \\
&\quad \times (z^* - e^{i\theta}\alpha)^n (z + e^{-i\theta}\beta^*)^n.
\end{aligned} \tag{99}$$

Change variables $z \rightarrow e^{-i\theta}z$, so the inner product is now

$$\begin{aligned}
\left\langle F_{\exp(i\theta)\alpha}^*(z) \middle| F_{\exp(i\theta)\beta}^*(z) \right\rangle &= \frac{1}{\pi} \frac{e^{-(|\alpha|^2 + |\beta|^2)/2}}{n!} \\
&\quad \times \int_{z \in \mathbb{C}} d^2 z e^{-[|z|^2 - \exp(-i\theta)\alpha^* \exp(i\theta)z^* - \exp(i\theta)\beta \exp(-i\theta)z]} \\
&\quad \times (e^{i\theta}z^* - e^{i\theta}\alpha)^n (e^{-i\theta}z + e^{-i\theta}\beta^*)^n \\
&= \frac{1}{\pi} \frac{e^{-(|\alpha|^2 + |\beta|^2)/2}}{n!} \int_{z \in \mathbb{C}} d^2 z e^{-(|z|^2 - \alpha^* z^* - \beta z)} \\
&\quad \times e^{ni\theta} e^{-ni\theta} (z^* - \alpha)^n (z + \beta^*)^n \\
&= \frac{1}{\pi} \frac{e^{-(|\alpha|^2 + |\beta|^2)/2}}{n!} \int_{z \in \mathbb{C}} d^2 z e^{-(|z|^2 - \alpha^* z^* - \beta z)} \\
&\quad \times (z^* - \alpha)^n (z + \beta^*)^n \\
&= \left\langle F_{\alpha}^*(z) \middle| F_{\beta}^*(z) \right\rangle
\end{aligned} \tag{100}$$

and the displaced Fock state kernel is rotational invariant.

D.5 Showing the displaced Fock state kernel is a radial kernel

From these translation and rotation invariance of the displaced Fock state kernel, can also show that

$$\begin{aligned} k(\mathcal{R}(\theta)(\boldsymbol{\alpha} - \boldsymbol{\beta})) &= k(\mathcal{R}(\theta)\boldsymbol{\alpha} - \mathcal{R}(\theta)\boldsymbol{\beta}) \\ &= k(\mathcal{R}(\theta)\boldsymbol{\alpha}, \mathcal{R}(\theta)\boldsymbol{\beta}) \\ &= k(\boldsymbol{\alpha}, \boldsymbol{\beta}) \\ &= k(\boldsymbol{\alpha} - \boldsymbol{\beta}), \end{aligned} \quad (101)$$

and therefore

$$k(\boldsymbol{\alpha}, \boldsymbol{\beta}) = k(|\boldsymbol{\alpha} - \boldsymbol{\beta}|) \quad (102)$$

it is a radial kernel.

Furthermore, the polynomial $P(\alpha, \beta)$ is a polynomial of $\alpha_1, \alpha_2, \beta_1$ and β_2 , but, there is no way of constructing

$$|\mathbf{s}| = \sqrt{(\alpha_1 - \beta_1)^2 + (\alpha_2 - \beta_2)^2} \quad (103)$$

out of such a polynomial. However there is a way of constructing

$$|\mathbf{s}|^2 = (\alpha_1 - \beta_1)^2 + (\alpha_2 - \beta_2)^2 = \alpha_1^2 + \alpha_2^2 + \beta_1^2 + \beta_2^2 - 2\alpha_1\beta_1 - 2\alpha_2\beta_2 \quad (104)$$

and therefore

$$k(\boldsymbol{\alpha}, \boldsymbol{\beta}) = k(|\boldsymbol{\alpha} - \boldsymbol{\beta}|^2) \quad (105)$$

D.6 The Fourier transform of the displaced Fock state kernel

Now define $\mathbf{s} := \boldsymbol{\alpha} - \boldsymbol{\beta}$, and use the facts that the displaced Fock state kernel is

$$k(\boldsymbol{\alpha}, \boldsymbol{\beta}) = k(|\mathbf{s}|^2) \quad (106)$$

and is the product of a Gaussian and a polynomial of degree $4n$ in \mathbf{s} , to write is as

$$k(|\mathbf{s}|) = e^{-|\mathbf{s}|^2} \sum_{j=0}^{2n} a_{2j} |\mathbf{s}|^{2j} \quad (107)$$

for an appropriate choice of $a_j \in \mathbb{R}$.

The two-dimensional Fourier transform can be easily calculated as

$$\begin{aligned} \frac{1}{2\pi} \int d^2s \ e^{i\mathbf{s} \cdot \boldsymbol{\omega}} k(\mathbf{s}) &= \frac{1}{2\pi} \sum_{j=0}^{2n} a_{2j} \int_0^\infty ds \int_0^{2\pi} d\theta \ s e^{is\omega \cos(\theta)} e^{-s^2} s^{2j} \\ &= \frac{1}{2\pi} \sum_{j=0}^{2n} a_{2j} \int_0^\infty ds \ e^{-s^2} s^{2j+1} J_0(\omega s) \\ &= \frac{1}{2\pi} \sum_{j=0}^{2n} a_{2j} \left[\frac{j!}{2} {}_1F_1 \left(1+j; 1; -\frac{\omega^2}{4} \right) \right] \end{aligned} \quad (108)$$

which can be simplified further using the hypergeometric identity in appendix C.2

$$\begin{aligned} \frac{1}{2\pi} \int d^2s \ e^{i\mathbf{s} \cdot \boldsymbol{\omega}} k(\mathbf{s}) &= \frac{1}{4\pi} \sum_{j=0}^{2n} j! a_{2j} e^{-\omega^2/4} \sum_{\ell=0}^j \binom{j}{\ell} \frac{1}{(1)_\ell} \left(-\frac{\omega^2}{4} \right)^\ell \\ &= \frac{e^{-\omega^2/4}}{4\pi} \sum_{j=0}^{2n} (j!)^2 a_{2j} \sum_{\ell=0}^j \frac{(-1)^\ell}{(\ell!)^2 (j-\ell)!} \left(\frac{\omega}{2} \right)^{2\ell} \end{aligned} \quad (109)$$

which is also the product of a Gaussian and a polynomial of degree $4n$ in ω .

D.7 Showing the displaced Fock state kernel integrates to π

In this section, we calculate the displaced Fock state kernel from the operator definition:

$$\hat{D}(\alpha) = e^{\alpha \hat{a}^\dagger - \alpha^* \hat{a}} = e^{-|\alpha|^2/2} e^{\alpha \hat{a}^\dagger} e^{-\alpha^* \hat{a}}. \quad (110)$$

Starting from

$$\begin{aligned} e^{\pm \alpha^* \hat{a}} |n\rangle &= \sum_{j=0}^{\infty} \frac{(\pm \alpha^*)^j \hat{a}^j}{j!} |n\rangle \\ &= |n\rangle + \sum_{j=1}^{\infty} \frac{(\pm \alpha^*)^j \hat{a}^j}{j!} |n\rangle \\ &= |n\rangle + \sum_{j=1}^n \frac{(\pm \alpha^*)^j}{j!} \prod_{\ell=1}^j \sqrt{n-\ell+1} |n-j\rangle. \end{aligned} \quad (111)$$

we calculate the inner product as

$$\begin{aligned} \langle n | \hat{D}^\dagger(\alpha) \hat{D}(\beta) | n \rangle &= e^{(-\alpha \beta^* + \alpha^* \beta)/2} \langle n | \hat{D}(\beta - \alpha) | n \rangle \\ &= e^{-|\beta - \alpha|^2/2} e^{i \operatorname{Im}(\alpha^* \beta)} \langle n | e^{(\beta - \alpha) \hat{a}^\dagger} e^{-(\beta - \alpha)^* \hat{a}} | n \rangle \\ &= e^{-|\beta - \alpha|^2/2} e^{i \operatorname{Im}(\alpha^* \beta)} \left(e^{(\beta - \alpha)^* \hat{a}} |n\rangle \right)^\dagger \left(e^{-(\beta - \alpha) \hat{a}} |n\rangle \right) \\ &= e^{-|\beta - \alpha|^2/2} e^{i \operatorname{Im}(\alpha^* \beta)} \left(\langle n | + \sum_{i=1}^n \frac{(\beta - \alpha)^i}{i!} \prod_{k=1}^i \sqrt{n-k+1} \langle n-i | \right) \\ &\quad \times \left(|n\rangle + \sum_{j=1}^n \frac{-(\beta - \alpha)^*^j}{j!} \prod_{\ell=1}^j \sqrt{n-\ell+1} |n-j\rangle \right) \\ &= e^{-|\beta - \alpha|^2/2} e^{i \operatorname{Im}(\alpha^* \beta)} \left(1 + \sum_{j=1}^n \frac{(\beta - \alpha)^j (-(\beta - \alpha)^*)^j}{(j!)^2} (\sqrt{n} \sqrt{n-1} \dots \sqrt{n-j+1})^2 \right) \\ &= e^{-|\beta - \alpha|^2/2} e^{i \operatorname{Im}(\alpha^* \beta)} \sum_{j=0}^n \frac{(-1)^j |\beta - \alpha|^{2j}}{(j!)^2} \frac{n!}{(n-j)!} \\ &= e^{-|\beta - \alpha|^2/2} e^{i \operatorname{Im}(\alpha^* \beta)} \sum_{j=0}^n \binom{n}{j} \frac{(-1)^j |\beta - \alpha|^{2j}}{j!} \end{aligned} \quad (112)$$

and the displaced Fock state kernel

$$k(\alpha, \beta) = \left| \langle n | \hat{D}^\dagger(\alpha) \hat{D}(\beta) | n \rangle \right|^2 = e^{-|\beta - \alpha|^2} \left(\sum_{j=0}^n \binom{n}{j} \frac{(-1)^j |\beta - \alpha|^{2j}}{j!} \right)^2. \quad (113)$$

Note that this is a much simpler form than that which we found Eq. (26), indicating that there may be a way to significantly simplify the general multi-mode kernel Eq. (46). We leave this exploration for future work.

Now define $\mathbf{s} := \boldsymbol{\alpha} - \boldsymbol{\beta} \in \mathbb{R}^2$ and integrate the kernel over all \mathbf{s}

$$\begin{aligned}
\int d^2s \, k(|\mathbf{s}|) &= \int_0^\infty ds \, s \int_0^{2\pi} d\theta \, e^{-s^2} \left(\sum_{j=0}^n \binom{n}{j} \frac{(-1)^j s^{2j}}{j!} \right)^2 \\
&= 2\pi \sum_{j=0}^n \sum_{k=0}^n \binom{n}{j} \binom{n}{k} \frac{(-1)^j}{j!} \frac{(-1)^k}{k!} \int_0^\infty ds \, e^{-s^2} s^{2(j+k)+1} \\
&= 2\pi \sum_{j=0}^n \sum_{k=0}^n \binom{n}{j} \binom{n}{k} \frac{(-1)^{j+k}}{j!k!} \left(\frac{\Gamma(1+j+k)}{2} \right) \\
&= \pi \sum_{j=0}^n \sum_{k=0}^n (-1)^{j+k} \binom{n}{j} \binom{n}{k} \binom{j+k}{k}. \tag{114}
\end{aligned}$$

The binomial coefficients can be further simplified by using the following properties for $k, n \in \mathbb{N}_0$, $m \in \mathbb{Z}$, and $x, y \in \mathbb{R}$ [50]:

$$\binom{x}{k} = \frac{x^{\underline{k}}}{k!} \tag{115a}$$

$$\binom{m}{k} = (-1)^k \binom{-m+k-1}{k} \tag{115b}$$

$$\binom{n}{k} = (-1)^{n-k} \binom{-k-1}{n-k} \quad k \leq n \tag{115c}$$

$$\binom{x+y}{n} = \sum_{k=0}^n \binom{x}{k} \binom{y}{n-k} \tag{115d}$$

where

$$x^{\underline{k}} = x(x-1)(x-2)\dots(x-k+1) \tag{116}$$

is the falling factorial.

With these properties, the integral becomes:

$$\begin{aligned}
\int d^2s \, k(|\mathbf{s}|) &= \pi \sum_{j=0}^n \sum_{k=0}^n (-1)^{j+k} \binom{n}{j} \binom{n}{k} \binom{j+k}{k} \\
&= \pi \sum_{j=0}^n \sum_{k=0}^n (-1)^{j+k} \binom{n}{j} \binom{n}{k} (-1)^{j+k-k} \binom{-(k+1)}{j} \quad (\text{Eq. (115c)}) \\
&= \pi \sum_{k=0}^n (-1)^k \binom{n}{k} \sum_{j=0}^n \binom{n}{n-j} \binom{-(k+1)}{j} \\
&= \pi \sum_{k=0}^n (-1)^k \binom{n}{k} \binom{n-(k+1)}{n} \quad (\text{Eq. (115d)}) \\
&= \pi \sum_{k=0}^n (-1)^k \binom{n}{k} (-1)^n \binom{k}{n} \quad (\text{Eq. (115b)}) \\
&= \pi \sum_{k=0}^n (-1)^{n+k} \binom{n}{k} \frac{k^{\underline{n}}}{n!} \quad (\text{Eq. (115a)}). \tag{117}
\end{aligned}$$

Since $0 \leq k \leq n$, the falling factorial becomes

$$k^{\underline{n}} = k(k-1)\dots(k-k)\dots(k-n+1) \tag{118}$$

which is zero unless $k = n$, so

$$\begin{aligned}
\int d^2s \, k(|s|) &= \pi \sum_{k=0}^n (-1)^{n+k} \binom{n}{k} \frac{k(k-1)\dots(k-n+1)}{n!} \delta_{k,n} \\
&= \pi (-1)^{2n} \binom{n}{n} \frac{n!}{n!} \\
&= \pi
\end{aligned} \tag{119}$$

for all $n \in \mathbb{N}_0$.

E Explicit calculation of the general m -mode CV kernel

In this section, we provide the details of the calculation of the general m -mode kernel (Eq. (46)).

The first step in calculating the m -mode kernel is to rewrite Eq. (44) to become a series of nested integrals each of the form of Eq. (84).

Starting from the general m -mode inner product,

$$\begin{aligned}
\langle F_{x_1}^* | F_{x_2}^* \rangle &= \frac{1}{\pi^m} \int_{\mathbf{z} \in \mathbb{C}^m} d^{2m}z \, e^{-|z|^2} F_{x_1}(z)^* F_{x_2}(z) \\
&= \frac{1}{\pi^m} \int_{\mathbf{z} \in \mathbb{C}^m} d^{2m}z \, e^{-|z|^2} \exp\left(-\frac{1}{2} \mathbf{z}^\dagger \mathbf{A}^{(1)*} \mathbf{z}^* + \mathbf{B}^{(1)\dagger} \mathbf{z}^* + C^{(1)*}\right) \\
&\quad \times \left(\sum_{i_1+i_2+\dots+i_m=n} \beta_i^{(1)*} (z_1^*)^{i_1} (z_2^*)^{i_2} \dots (z_n^*)^{i_n} \right) \\
&\quad \times \exp\left(-\frac{1}{2} \mathbf{z}^\top \mathbf{A}^{(2)} \mathbf{z} + \mathbf{B}^{(2)\top} \mathbf{z} + C^{(2)}\right) \left(\sum_{j_1+j_2+\dots+j_n=n} \beta_j^{(2)} z_1^{j_1} z_2^{j_2} \dots z_n^{j_n} \right) \\
&= \frac{1}{\pi^m} \int_{\mathbf{z} \in \mathbb{C}^m} d^{2m}z \, \exp\left(-|z|^2 - \frac{1}{2} \mathbf{z}^\dagger \mathbf{A}^{(1)*} \mathbf{z}^* - \frac{1}{2} \mathbf{z}^\top \mathbf{A}^{(2)} \mathbf{z} + \mathbf{B}^{(1)\dagger} \mathbf{z}^* + \mathbf{B}^{(2)\top} \mathbf{z} + C^{(1)*} + C^{(2)}\right) \\
&\quad \times \left(\sum_{i_1+i_2+\dots+i_m=n} \sum_{j_1+j_2+\dots+j_n=n} \beta_i^{(1)*} \beta_j^{(2)} (z_1^*)^{i_1} z_1^{j_1} (z_2^*)^{i_2} z_2^{j_2} \dots (z_n^*)^{i_n} z_n^{j_n} \right).
\end{aligned} \tag{120}$$

Unsurprisingly the integrand is also of the form

$$\exp[Q(\mathbf{z})] \times P(\mathbf{z}) \tag{121}$$

i.e. the product of a Gaussian and a polynomial.

Similar to the calculation of the displaced Fock state kernel, we set $z_j = x_{2j-1} + ix_{2j}$ for each $j \in [1, m]$. After some algebra, which we detail below, this substitution will allow for Eq. (120) to be written as a nested set of integrals, each of the form of Eq. (84).

First simplify the Gaussian part of the integrand:

$$\begin{aligned}
Q(\mathbf{z}) &= \left(C^{(1)*} + C^{(2)}\right) + \sum_{j=1}^m -(x_{2j-1}^2 + x_{2j}^2) - \frac{A_{j,j}^{(1)*}}{2} (x_{2j-1} - ix_{2j})^2 - \frac{A_{j,j}^{(2)}}{2} (x_{2j-1} + ix_{2j})^2 \\
&\quad + (x_{2j-1} - ix_{2j}) \left(B_j^{(1)*} - \sum_{k=j+1}^m \frac{A_{j,k}^{(1)*} + A_{k,j}^{(1)*}}{2} (x_{2j-1} - ix_{2j}) \right) \\
&\quad + (x_{2j-1} + ix_{2j}) \left(B_j^{(2)} - \sum_{k=j+1}^m \frac{A_{j,k}^{(2)} + A_{k,j}^{(2)}}{2} (x_{2j-1} + ix_{2j}) \right) \\
&= \left(C^{(1)*} + C^{(2)}\right) + \sum_{j=1}^m - \left(1 + \frac{A_{j,j}^{(1)*}}{2} + \frac{A_{j,j}^{(2)}}{2} \right) x_{2j-1}^2 - \left(1 - \frac{A_{j,j}^{(1)*}}{2} - \frac{A_{j,j}^{(2)}}{2} \right) x_{2j}^2 \\
&\quad + x_{2j-1} \left(\left(B_j^{(1)*} + B_j^{(2)} \right) - i \left(A_{j,j}^{(1)*} - A_{j,j}^{(2)} \right) x_{2j} \right. \\
&\quad \left. - \frac{1}{2} \sum_{k=j+1}^m \left(A_{j,k}^{(1)*} + A_{k,j}^{(1)*} + A_{j,k}^{(2)} + A_{k,j}^{(2)} \right) x_{2k-1} - i \left(A_{j,k}^{(1)*} + A_{k,j}^{(1)*} - A_{j,k}^{(2)} - A_{k,j}^{(2)} \right) x_{2k} \right) \\
&\quad - ix_{2j} \left(\left(B_j^{(1)*} - B_j^{(2)} \right) \right. \\
&\quad \left. - \frac{1}{2} \sum_{k=j+1}^m \left(A_{j,k}^{(1)*} + A_{k,j}^{(1)*} - A_{j,k}^{(2)} - A_{k,j}^{(2)} \right) x_{2k-1} - i \left(A_{j,k}^{(1)*} + A_{k,j}^{(1)*} + A_{j,k}^{(2)} + A_{k,j}^{(2)} \right) x_{2k} \right) \\
&= \left(C^{(1)*} + C^{(2)}\right) + \sum_{j=1}^{2m} -a_{0,j} x_j^2 + x_j \left(b_{0,j} + \sum_{k=j+1}^{2m} d_{0,j,k} x_k \right) \tag{122}
\end{aligned}$$

where for odd j

$$\begin{aligned}
a_{0,j} &:= \left(1 + \frac{\left(A_{(j+1)/2, (j+1)/2}^{(1)} \right)^*}{2} + \frac{A_{(j+1)/2, (j+1)/2}^{(2)}}{2} \right) \\
b_{0,j} &:= \left(B_{(j+1)/2}^{(1)} \right)^* + B_{(j+1)/2}^{(2)} \\
d_{0,j,k} &:= \begin{cases} -i \left[\left(A_{(j+1)/2, (j+1)/2}^{(1)} \right)^* - A_{(j+1)/2, (j+1)/2}^{(2)} \right], & k = j+1 \\ -\frac{1}{2} \left[\left(A_{(j+1)/2, (k+1)/2}^{(1)} + A_{(k+1)/2, (j+1)/2}^{(1)} \right)^* + A_{(j+1)/2, (k+1)/2}^{(2)} + A_{(k+1)/2, (j+1)/2}^{(2)} \right], & k \geq j+2, \text{ } k \text{ odd} \\ \frac{i}{2} \left[\left(A_{(j+1)/2, k/2}^{(1)} + A_{k/2, (j+1)/2}^{(1)} \right)^* - A_{(j+1)/2, k/2}^{(2)} - A_{k/2, (j+1)/2}^{(2)} \right], & k \geq j+3, \text{ } k \text{ even} \end{cases} \tag{123}
\end{aligned}$$

and for even j

$$\begin{aligned}
a_{0,j} &:= \left(1 - \frac{\left(A_{j/2,j/2}^{(1)} \right)^*}{2} - \frac{A_{j/2,j/2}^{(2)}}{2} \right) \\
b_{0,j} &:= -i \left[\left(B_{j/2}^{(1)} \right)^* + B_{j/2}^{(2)} \right] \\
d_{0,j,k} &:= \begin{cases} \frac{i}{2} \left[\left(A_{j/2,(k+1)/2}^{(1)} + A_{(k+1)/2,j/2}^{(1)} \right)^* - A_{j/2,(k+1)/2}^{(2)} - A_{(k+1)/2,j/2}^{(2)} \right], & k \geq j+1, \text{ } k \text{ odd} \\ \frac{1}{2} \left[\left(A_{j/2,k/2}^{(1)} + A_{k/2,j/2}^{(1)} \right)^* + A_{j/2,k/2}^{(2)} + A_{k/2,j/2}^{(2)} \right], & k \geq j+2, \text{ } k \text{ even.} \end{cases}
\end{aligned} \tag{124}$$

Next, simplify the polynomial part of the integrand:

$$\begin{aligned}
P(\mathbf{z}) &= \sum_{i_1+\dots+i_m=n} \sum_{j_1+\dots+j_m=n} \beta_{\mathbf{i}}^{(1)*} \beta_{\mathbf{j}}^{(2)} \prod_{k=1}^m (x_{2k-1} - ix_{2k})^{i_k} (x_{2k-1} + ix_{2k})^{j_k} \\
&= \sum_{i_1+\dots+i_m=n} \sum_{j_1+\dots+j_m=n} \beta_{\mathbf{i}}^{(1)*} \beta_{\mathbf{j}}^{(2)} \prod_{k=1}^m \left(\sum_{p_k=0}^{i_k} \sum_{q_k=0}^{j_k} \binom{i_k}{p_k} \binom{j_k}{q_k} (-i)^{p_k} (i)^{q_k} x_{2k-1}^{i_k+j_k-p_k-q_k} x_{2k}^{p_k+q_k} \right) \\
&= \sum_{i_1+\dots+i_m=n} \sum_{j_1+\dots+j_m=n} \beta_{\mathbf{i}}^{(1)*} \beta_{\mathbf{j}}^{(2)} \\
&\quad \times \sum_{p_1=0}^{i_1} \sum_{q_1=0}^{j_1} \sum_{p_2=0}^{i_2} \sum_{q_2=0}^{j_2} \dots \sum_{p_m=0}^{i_m} \sum_{q_m=0}^{j_m} \prod_{k=1}^m \binom{i_k}{p_k} \binom{j_k}{q_k} (-i)^{p_k} (i)^{q_k} x_{2k-1}^{i_k+j_k-p_k-q_k} x_{2k}^{p_k+q_k} \\
&= \sum_{i_1+\dots+i_m=n} \sum_{j_1+\dots+j_m=n} \beta_{\mathbf{i}}^{(1)*} \beta_{\mathbf{j}}^{(2)} \sum_{\mathbf{p}=\mathbf{0}}^{\mathbf{i}} \sum_{\mathbf{q}=\mathbf{0}}^{\mathbf{j}} \prod_{k=1}^{2m} g_{0,k} x_k^{r_{0,k}}
\end{aligned} \tag{125}$$

where

$$\begin{aligned}
\sum_{\mathbf{p}=\mathbf{0}}^{\mathbf{i}} &= \sum_{p_1=0}^{i_1} \sum_{p_2=0}^{i_2} \dots \sum_{p_m=0}^{i_m} \\
\sum_{\mathbf{q}=\mathbf{0}}^{\mathbf{j}} &= \sum_{q_1=0}^{j_1} \sum_{q_2=0}^{j_2} \dots \sum_{q_m=0}^{j_m} \\
g_{0,k} &:= \begin{cases} 1, & k \text{ odd} \\ \binom{i_{k/2}}{p_{k/2}} \binom{j_{k/2}}{q_{k/2}} (-i)^{p_{k/2}} (i)^{q_{k/2}}, & k \text{ even} \end{cases} \\
r_{0,k} &:= \begin{cases} i_{(k+1)/2} + j_{(k+1)/2} - p_{(k+1)/2} - q_{(k+1)/2}, & k \text{ odd} \\ p_{k/2} + q_{k/2}, & k \text{ even.} \end{cases}
\end{aligned} \tag{126}$$

Therefore, the m -mode inner product can be written as:

$$\begin{aligned}
\langle F_{\mathbf{x}_1}^* | F_{\mathbf{x}_2}^* \rangle &= \frac{e^{C^{(1)*} + C^{(2)}}}{\pi^m} \sum_{i_1+\dots+i_m=n} \sum_{j_1+\dots+j_m=n} \beta_{\mathbf{i}}^{(1)*} \beta_{\mathbf{j}}^{(2)} \sum_{\mathbf{p}=\mathbf{0}}^{\mathbf{i}} \sum_{\mathbf{q}=\mathbf{0}}^{\mathbf{j}} \\
&\quad \times \int_{\mathbf{x} \in \mathbb{R}^{2m}} d^{2m}x \exp \left[\sum_{j=1}^{2m} -a_{0,j} x_j^2 + x_j \left(b_{0,j} + \sum_{k=j+1}^{2M} d_{0,j,k} x_k \right) \right] \\
&\quad \times \left(\prod_{k=1}^{2m} g_{0,k} x_k^{r_{0,k}} \right)
\end{aligned} \tag{127}$$

which is in the required form.

Now we can carry out the integrations starting with the x_1 integral, which is of the form Eq. (84):

$$\begin{aligned}
\langle F_{x_1}^* | F_{x_2}^* \rangle &= \frac{e^{C^{(1)*} + C^{(2)}}}{\pi^m} \sum_{i_1 + \dots + i_m = n} \sum_{j_1 + \dots + j_m = n} \beta_i^{(1)*} \beta_j^{(2)} \\
&\quad \times \sum_{p=0}^i \sum_{q=0}^j \int_{-\infty}^{\infty} dx_{2m} \int_{-\infty}^{\infty} dx_{2m-1} \cdots \int_{-\infty}^{\infty} dx_2 \\
&\quad \times \left\{ g_{0,1} \int_{-\infty}^{\infty} dx_1 \exp \left[-a_{0,1} x_1^2 + x_1 \left(b_{0,1} + \sum_{k=2}^{2m} d_{0,1,k} x_k \right) \right] x_1^{r_{0,1}} \right\} \\
&\quad \times \exp \left[\sum_{j=2}^{2m} -a_{0,j} x_j^2 + x_j \left(b_{0,j} + \sum_{k=j+1}^{2m} d_{0,j,k} x_k \right) \right] \left(\prod_{k=2}^{2m} g_{0,k} x_k^{r_{0,k}} \right) \\
&= \frac{e^{C^{(1)*} + C^{(2)}}}{\pi^m} \sum_{i_1 + \dots + i_m = n} \sum_{j_1 + \dots + j_m = n} \beta_i^{(1)*} \beta_j^{(2)} \\
&\quad \times \sum_{p=0}^i \sum_{q=0}^j \int_{-\infty}^{\infty} dx_{2m} \int_{-\infty}^{\infty} dx_{2m-1} \cdots \int_{-\infty}^{\infty} dx_2 \\
&\quad \times \left\{ g_{0,1} a_{0,1}^{-(r_{0,1}+1)/2} \exp \left[\frac{1}{4a_{0,1}} \left(b_{0,1} + \sum_{k=2}^{2m} d_{0,1,k} x_k \right)^2 \right] \right. \\
&\quad \times \left. \sum_{s_1=0}^{r_{0,1}} \gamma_{r_{0,1}, s_1} \left[\frac{1}{\sqrt{a_{0,1}}} \left(b_{0,1} + \sum_{k=2}^{2m} d_{0,1,k} x_k \right) \right]^{s_1} \right\} \\
&\quad \times \exp \left[\sum_{j=2}^{2m} -a_{0,j} x_j^2 + x_j \left(b_{0,j} + \sum_{k=j+1}^{2m} d_{0,j,k} x_k \right) \right] \left(\prod_{k=2}^{2m} g_{0,k} x_k^{r_{0,k}} \right) \\
&= \frac{e^{C^{(1)*} + C^{(2)}}}{\pi^m} \sum_{i_1 + \dots + i_m = n} \sum_{j_1 + \dots + j_m = n} \beta_i^{(1)*} \beta_j^{(2)} \\
&\quad \times \sum_{p=0}^i \sum_{q=0}^j \int_{-\infty}^{\infty} dx_{2m} \int_{-\infty}^{\infty} dx_{2m-1} \cdots \int_{-\infty}^{\infty} dx_2 \exp \left[\frac{1}{4a_{0,1}} \left(b_{0,1} + \sum_{k=2}^{2m} d_{0,1,k} x_k \right)^2 \right] \\
&\quad \times \exp \left[\sum_{j=2}^{2m} -a_{0,j} x_j^2 + x_j \left(b_{0,j} + \sum_{k=j+1}^{2m} d_{0,j,k} x_k \right) \right] \\
&\quad \times \left[a_{0,1}^{-(r_{0,1}+1)/2} \sum_{s_1=0}^{r_{0,1}} \gamma_{r_{0,1}, s_1} \left[\frac{1}{\sqrt{a_{0,1}}} \left(b_{0,1} + \sum_{k=2}^{2m} d_{0,1,k} x_k \right) \right]^{s_1} \right] \left(\prod_{k=2}^{2m} g_{0,k} x_k^{r_{0,k}} \right)
\end{aligned} \tag{128}$$

where we also use the fact that $g_{0,1} = 1$ (Eq. (126)).

Next, the goal is to simplify the integrand so that the x_2 integral is of the form of Eq. (84).

Start by simplifying the exponential part:

$$\begin{aligned}
& \frac{1}{4a_{0,1}} \left(b_{0,1} + \sum_{j=2}^{2m} d_{0,1,j} x_j \right)^2 + \sum_{j=2}^{2m} -a_{0,j} x_j^2 + x_j \left(b_{0,j} + \sum_{k=j+1}^{2m} d_{0,j,k} x_k \right) \\
&= \frac{b_{0,1}^2}{4a_{0,1}} + \sum_{j=2}^{2m} - \left(a_{0,j} - \frac{d_{0,1,j}^2}{4a_{0,1}} \right) x_j^2 + x_j \left[\left(b_{0,j} + \frac{b_{0,1} d_{0,1,j}}{2a_{0,1}} \right) \right. \\
&\quad \left. + \sum_{k=j+1}^{2m} \left(d_{0,j,k} + \frac{d_{0,1,j} d_{0,1,k}}{2a_{0,1}} \right) x_k \right] \\
&= \frac{b_{0,1}^2}{4a_{0,1}} + \sum_{j=2}^{2m} -a_{1,j} x_j^2 + x_j \left(b_{1,j} + \sum_{k=j+1}^{2m} d_{1,j,k} x_k \right) \tag{129}
\end{aligned}$$

where

$$\begin{aligned}
a_{1,j} &:= a_{0,j} - \frac{d_{0,1,j}^2}{4a_{0,1}} \\
b_{1,j} &:= b_{0,j} + \frac{b_{0,1} d_{0,1,j}}{2a_{0,1}} \\
d_{1,j,k} &:= d_{0,j,k} + \frac{d_{0,1,j} d_{0,1,k}}{2a_{0,1}}. \tag{130}
\end{aligned}$$

Then use the multinomial expansion,

$$(x_1 + x_2 + \cdots + x_m)^n = \sum_{\substack{i_1, i_2, \dots, i_m \geq 0 \\ i_1 + i_2 + \cdots + i_m = n}} \frac{n!}{i_1! i_2! \cdots i_m!} x_1^{i_1} x_2^{i_2} \cdots x_m^{i_m} \tag{131}$$

to simplify the polynomial part:

$$\begin{aligned}
& \left[a_{0,1}^{-\frac{(r_{0,1}+1)}{2}} \sum_{s_1=0}^{r_{0,1}} \gamma_{r_{0,1}, s_1} \left(\frac{1}{\sqrt{a_{0,1}}} \right)^{s_1} \left(b_{0,1} + \sum_{j=2}^{2m} d_{0,1,j} x_j \right)^{s_1} \right] \left(\prod_{k=2}^{2m} g_{0,k} x_k^{r_{0,k}} \right) \\
&= \left[\sum_{s_1=0}^{r_{0,1}} \frac{\gamma_{r_{0,1}, s_1}}{a_{0,1}^{\frac{(r_{0,1}+s_1+1)}{2}}} \sum_{t_1=0}^{s_1} \binom{s_1}{t_1} b_{0,1}^{s_1-t_1} \left(\sum_{j=2}^{2m} d_{0,1,j} x_j \right)^{t_1} \right] \left(\prod_{k=2}^{2m} g_{0,k} x_k^{r_{0,k}} \right) \\
&= \left[\sum_{s_1=0}^{r_{0,1}} \frac{\gamma_{r_{0,1}, s_1}}{a_{0,1}^{\frac{(r_{0,1}+s_1+1)}{2}}} \sum_{t_1=0}^{s_1} \binom{s_1}{t_1} b_{0,1}^{s_1-t_1} \right. \\
&\quad \times \left(\sum_{u_{1,2}+u_{1,3}+\cdots+u_{1,2m}=t_1} \frac{t_1!}{u_{1,2}! u_{1,3}! \cdots u_{1,2m}!} \prod_{k=2}^{2m} d_{0,1,k}^{u_{1,k}} x_k^{u_{1,k}} \right) \left. \right] \\
&\quad \times \left(\prod_{k=2}^{2m} g_{0,k} x_k^{r_{0,k}} \right) \\
&= \sum_{s_1=0}^{r_{0,1}} \frac{\gamma_{r_{0,1}, s_1}}{a_{0,1}^{\frac{(r_{0,1}+s_1+1)}{2}}} \sum_{t_1=0}^{s_1} \frac{s_1!}{(s_1-t_1)!} b_{0,1}^{s_1-t_1} \sum_{u_{1,2}+\cdots+u_{1,2m}=t_1} \prod_{k=2}^{2m} \frac{g_{0,k} d_{0,1,k}^{u_{1,k}}}{u_{1,k}!} x_k^{u_{1,k}+r_{0,k}} \\
&= \sum_{s_1=0}^{r_{0,1}} \frac{\gamma_{r_{0,1}, s_1}}{a_{0,1}^{\frac{(r_{0,1}+s_1+1)}{2}}} \sum_{t_1=0}^{s_1} \frac{s_1!}{(s_1-t_1)!} b_{0,1}^{s_1-t_1} \sum_{u_{1,2}+\cdots+u_{1,2m}=t_1} \prod_{k=2}^{2m} g_{1,k} x_k^{r_{1,k}} \tag{132}
\end{aligned}$$

where for $k \geq 2$

$$\begin{aligned} g_{1,k} &:= \frac{g_{0,k} d_{0,1,k}^{u_{1,k}}}{u_{1,k}!} \\ r_{1,k} &:= r_{0,k} + u_{1,k} \end{aligned} \tag{133}$$

Therefore the m -mode inner product becomes

$$\begin{aligned} \langle F_{x_1}^* | F_{x_2}^* \rangle &= \exp \left(C^{(1)*} + C^{(2)} + \frac{b_{0,1}^2}{4a_{0,1}} \right) \sum_{i_1+\dots+i_m=n} \sum_{j_1+\dots+j_m=n} \beta_{\mathbf{i}}^{(1)*} \beta_{\mathbf{j}}^{(2)} \\ &\quad \times \sum_{\mathbf{p}=\mathbf{0}}^{\mathbf{i}} \sum_{\mathbf{q}=\mathbf{0}}^{\mathbf{j}} \sum_{s_1=0}^{r_{0,1}} \frac{\gamma_{r_{0,1},s_1}}{a_{0,1}^{(r_{0,1}+s_1+1)/2}} \sum_{t_1=0}^{s_1} \frac{s_1!}{(s_1-t_1)!} b_{0,1}^{s_1-t_1} \sum_{u_{1,2}+\dots+u_{1,2m}=t_1} \\ &\quad \times \int_{-\infty}^{\infty} dx_{2m} \cdots \int_{-\infty}^{\infty} dx_2 \exp \left[\sum_{j=2}^{2m} -a_{1,j} x_j^2 + x_j \left(b_{1,j} + \sum_{k=j+1}^{2m} d_{1,j,k} x_k \right) \right] \left(\prod_{k=2}^{2m} g_{1,k} x_k^{r_{1,k}} \right) \\ &= \exp \left(C^{(1)*} + C^{(2)} + \frac{b_{0,1}^2}{4a_{0,1}} \right) \sum_{i_1+\dots+i_m=n} \sum_{j_1+\dots+j_m=n} \beta_{\mathbf{i}}^{(1)*} \beta_{\mathbf{j}}^{(2)} \\ &\quad \times \sum_{\mathbf{p}=\mathbf{0}}^{\mathbf{i}} \sum_{\mathbf{q}=\mathbf{0}}^{\mathbf{j}} \sum_{s_1=0}^{r_{0,1}} \frac{\gamma_{r_{0,1},s_1}}{a_{0,1}^{(r_{0,1}+s_1+1)/2}} \sum_{t_1=0}^{s_1} \frac{s_1!}{(s_1-t_1)!} b_{0,1}^{s_1-t_1} \sum_{u_{1,2}+\dots+u_{1,2m}=t_1} \int_{-\infty}^{\infty} dx_{2m} \cdots \int_{-\infty}^{\infty} dx_3 \\ &\quad \times \left\{ g_{1,2} \int_{-\infty}^{\infty} dx_2 \exp \left[-a_{1,2} x_2^2 + x_2 \left(b_{1,2} + \sum_{k=3}^{2m} d_{1,2,k} x_k \right) \right] x_2^{r_{1,2}} \right\} \\ &\quad \times \exp \left[\sum_{j=3}^{2m} -a_{1,j} x_j^2 + x_j \left(b_{1,j} + \sum_{k=j+1}^{2m} d_{1,j,k} x_k \right) \right] \left(\prod_{k=3}^{2m} g_{1,k} x_k^{r_{1,k}} \right) \end{aligned}$$

$$\begin{aligned}
&= \exp \left(C^{(1)*} + C^{(2)} + \frac{b_{0,1}^2}{4a_{0,1}} \right) \sum_{i_1+\dots+i_m=n} \sum_{j_1+\dots+j_m=n} \beta_i^{(1)*} \beta_j^{(2)} \\
&\quad \times \sum_{\mathbf{p}=\mathbf{0}}^{\mathbf{i}} \sum_{\mathbf{q}=\mathbf{0}}^{\mathbf{j}} \sum_{s_1=0}^{r_{0,1}} \frac{\gamma_{r_{0,1},s_1}}{a_{0,1}^{(r_{0,1}+s_1+1)/2}} \sum_{t_1=0}^{s_1} \frac{s_1!}{(s_1-t_1)!} b_{0,1}^{s_1-t_1} \sum_{u_{1,2}+\dots+u_{1,2m}=t_1} \int_{-\infty}^{\infty} dx_{2m} \cdots \int_{-\infty}^{\infty} dx_3 \\
&\quad \times \left\{ g_{1,2} a_{1,2}^{-(r_{1,2}+1)/2} \exp \left[\frac{1}{4a_{1,2}} \left(b_{1,2} + \sum_{k=3}^{2m} d_{1,2,k} x_k \right) \right]^2 \right. \\
&\quad \times \sum_{s_2=0}^{r_{1,2}} \gamma_{r_{1,2},s_2} \left[\frac{1}{\sqrt{a_{1,2}}} \left(b_{1,2} + \sum_{k=3}^{2m} d_{1,2,k} x_k \right) \right]^{s_2} \Big\} \\
&\quad \times \exp \left[\sum_{j=3}^{2m} -a_{1,j} x_j^2 + x_j \left(b_{1,j} + \sum_{k=j+1}^{2m} d_{1,j,k} x_k \right) \right] \left(\prod_{k=3}^{2m} g_{1,k} x_k^{r_{1,k}} \right) \\
&= \exp \left(C^{(1)*} + C^{(2)} + \frac{b_{0,1}^2}{4a_{0,1}} + \frac{b_{1,2}^2}{4a_{1,2}} \right) \sum_{i_1+\dots+i_m=n} \sum_{j_1+\dots+j_m=n} \beta_i^{(1)*} \beta_j^{(2)} \\
&\quad \times \sum_{\mathbf{p}=\mathbf{0}}^{\mathbf{i}} \sum_{\mathbf{q}=\mathbf{0}}^{\mathbf{j}} \sum_{s_1=0}^{r_{0,1}} \frac{\gamma_{r_{0,1},s_1}}{a_{0,1}^{(r_{0,1}+s_1+1)/2}} \sum_{t_1=0}^{s_1} \frac{s_1!}{(s_1-t_1)!} b_{0,1}^{s_1-t_1} \sum_{u_{1,2}+\dots+u_{1,2m}=t_1} g_{1,2} \\
&\quad \times \sum_{s_2=0}^{r_{1,2}} \frac{\gamma_{r_{1,2},s_2}}{a_{1,2}^{(r_{1,2}+s_2+1)/2}} \sum_{t_2=0}^{s_2} \frac{s_2!}{(s_2-t_2)!} b_{1,2}^{s_2-t_2} \sum_{u_{2,3}+\dots+u_{2,2m}=t_2} \\
&\quad \times \int_{-\infty}^{\infty} dx_{2m} \cdots \int_{-\infty}^{\infty} dx_3 \exp \left[\sum_{j=3}^{2m} -a_{2,j} x_j^2 + x_j \left(b_{2,j} + \sum_{k=j+1}^{2m} d_{2,j,k} x_k \right) \right] \left(\prod_{k=3}^{2m} g_{2,k} x_k^{r_{2,k}} \right) \\
&\hspace{25em} (134)
\end{aligned}$$

where the last equality results from following a similar simplification as was done following the x_1 integral and we define:

$$\begin{aligned}
a_{2,j} &:= a_{1,j} - \frac{d_{1,2,j}^2}{4a_{1,2}} \\
b_{2,j} &:= b_{1,j} + \frac{b_{1,2} d_{1,2,j}}{2a_{1,2}} \\
d_{2,j,k} &:= d_{1,j,k} + \frac{d_{1,2,j} d_{1,2,k}}{2a_{1,2}} \\
g_{2,k} &:= \frac{g_{1,k} d_{1,2,k}^{u_{2,k}}}{u_{2,k}!} \\
r_{2,k} &:= r_{1,k} + u_{2,k}.
\end{aligned} \tag{135}$$

The next $2m - 2$ integrals can be evaluated iteratively following the same steps as

above which results in the following closed form of the m -mode inner product:

$$\begin{aligned}
\langle F_{x_1}^* | F_{x_2}^* \rangle &= \frac{1}{\pi^m} \exp \left(C^{(1)*} + C^{(2)} + \sum_{j=1}^{2m} \frac{b_{j-1,j}^2}{4a_{j-1,j}} \right) \sum_{i_1+\dots+i_m=n} \sum_{j_1+\dots+j_m=n} \beta_i^{(1)*} \beta_j^{(2)} \\
&\times \sum_{p=0}^i \sum_{q=0}^j \prod_{\ell=1}^{2m-1} \left(\sum_{s_\ell=0}^{r_{\ell-1,\ell}} \frac{\gamma_{r_{\ell-1,\ell},s_\ell}}{a_{\ell-1,\ell}^{(r_{\ell-1,\ell}+s_\ell+1)/2}} \sum_{t_\ell=0}^{s_\ell} \frac{s_\ell!}{(s_\ell-t_\ell)!} b_{\ell-1,\ell}^{s_\ell-t_\ell} \right. \\
&\times \left. \sum_{u_{\ell,\ell+1}+\dots+u_{\ell,2m}=t_\ell} g_{\ell,\ell+1} \right) \left(\sum_{s_{2m}=0}^{r_{2m-1,2m}} \frac{\gamma_{r_{2m-1,2m},s_{2m}}}{a_{2m-1,2m}^{(r_{2m-1,2m}+s_{2m}+1)/2}} b_{2m-1,2m}^{s_{2m}} \right)
\end{aligned} \tag{136}$$

where

$$\begin{aligned}
a_{i,j} &:= a_{i-1,j} - \frac{d_{i-1,i,j}^2}{4a_{i-1,i}} \\
b_{i,j} &:= b_{i-1,j} + \frac{b_{i-1,i}d_{i-1,i,j}}{2a_{i-1,i}} \\
d_{i,j,k} &:= d_{i-1,j,k} + \frac{d_{i-1,i,j}d_{i-1,i,k}}{2a_{i-1,i}} \\
g_{i,k} &:= \frac{g_{i-1,k}d_{i-1,i,k}^{u_{i,k}}}{u_{i,k}!} \\
r_{i,k} &:= r_{i-1,k} + u_{i,k}.
\end{aligned} \tag{137}$$

are defined recursively and the $\gamma_{r,s}$'s are defined in Eq. (27). We note that this expression is still a product of Gaussian and a polynomial of degree $2n$.

F Approximating CV kernels of infinite stellar rank

In this section we will show that kernels formed from pure states of infinite stellar rank can be approximated arbitrarily well by kernels of finite stellar rank.

CV states of infinite stellar rank can be approximated arbitrarily well in trace distance by states of finite stellar rank [33]. That is

$$T(|\psi\rangle\langle\psi|, |F\rangle\langle F|) \leq \epsilon \tag{138}$$

where we use $|\psi\rangle$ to denote a state of infinite stellar rank and $|F\rangle$ to denote a state of finite stellar rank. Since we are considering pure states, the trace distance can be easily expressed in terms of the inner product

$$T(|\psi\rangle\langle\psi|, |F\rangle\langle F|) = \sqrt{1 - |\langle\psi|F\rangle|^2} \leq \epsilon \implies 1 - |\langle\psi|F\rangle|^2 \leq \epsilon^2. \tag{139}$$

Now since

$$\langle\psi|F\rangle = e^{i\theta} |\langle\psi|F\rangle| \tag{140}$$

where $\theta \in [0, 2\pi)$ is the phase, we can define a new state with the same stellar rank as $|F\rangle$ as

$$|\tilde{F}\rangle := e^{-i\theta} |F\rangle \tag{141}$$

so that

$$\langle\psi|\tilde{F}\rangle = e^{-i\theta} \langle\psi|F\rangle = e^{-i\theta} (e^{i\theta} |\langle\psi|F\rangle|) = |\langle\psi|F\rangle|. \tag{142}$$

Also note that for any state $|\phi\rangle$,

$$|\langle\phi|\tilde{F}\rangle| = \sqrt{\langle\phi|\tilde{F}\rangle\langle\tilde{F}|\phi\rangle} = \sqrt{e^{-i\theta}\langle\phi|F\rangle e^{i\theta}\langle F|\phi\rangle} = \sqrt{\langle\phi|F\rangle\langle F|\phi\rangle} = |\langle\phi|F\rangle| \quad (143)$$

and

$$\begin{aligned} |\langle\psi - \tilde{F}|\phi\rangle| &\leq \sqrt{\langle\psi - \tilde{F}|\psi - \tilde{F}\rangle\langle\phi|\phi\rangle} && \text{(Cauchy-Schwarz)} \\ &= \sqrt{\langle\psi - \tilde{F}|\psi - \tilde{F}\rangle} \\ &= \sqrt{\langle\psi|\psi\rangle - \langle\psi|\tilde{F}\rangle - \langle\tilde{F}|\psi\rangle + \langle\tilde{F}|\tilde{F}\rangle} \\ &= \sqrt{2 - 2|\langle\psi|F\rangle|} && \text{(Eq. (142))} \\ &\leq \sqrt{2 - 2|\langle\psi|F\rangle|^2} && \left(\text{since } |z| \leq 1 \implies |z| \geq |z|^2\right) \\ &\leq \sqrt{2}\epsilon. && (144) \end{aligned}$$

Next stating from

$$T(|\psi_1\rangle\langle\psi_1|, |F_1\rangle\langle F_1|) \leq \epsilon \quad (145)$$

we will bound the inner product between the state of infinite stellar rank and another state of finite stellar rank.

$$\begin{aligned} |\langle\psi_1|F_2\rangle| &= |\langle\psi_1 - \tilde{F}_1 + \tilde{F}_1|F_2\rangle| \\ &= |\langle\psi_1 - \tilde{F}_1|F_2\rangle + \langle\tilde{F}_1|F_2\rangle| \\ &\leq |\langle\psi_1 - \tilde{F}_1|F_2\rangle| + |\langle\tilde{F}_1|F_2\rangle| \\ &\leq \sqrt{2}\epsilon + |\langle F_1|F_2\rangle|. && \text{(Eqs. (143) \& (144))} \end{aligned} \quad (146)$$

Therefore

$$|\langle\psi_1|F_2\rangle| - |\langle F_1|F_2\rangle| \leq \sqrt{2}\epsilon. \quad (147)$$

Similarly, we can show

$$\begin{aligned} |\langle F_1|F_2\rangle| &= |\langle\tilde{F}_1|F_2\rangle| \\ &= |\langle\tilde{F}_1 - \psi_1 + \psi_1|F_2\rangle| \\ &= |\langle\tilde{F}_1 - \psi_1|F_2\rangle + \langle\psi_1|F_2\rangle| \\ &\leq |\langle\tilde{F}_1 - \psi_1|F_2\rangle| + |\langle\psi_1|F_2\rangle| \\ &\leq \sqrt{2}\epsilon + |\langle\psi_1|F_2\rangle|. && \text{(Eq. (144))} \end{aligned} \quad (148)$$

Therefore

$$|\langle F_1|F_2\rangle| - |\langle\psi_1|F_2\rangle| \leq \sqrt{2}\epsilon \quad (149)$$

and combining Eqs. (147) and (149) gives

$$\left| |\langle\psi_1|F_2\rangle| - |\langle F_1|F_2\rangle| \right| \leq \sqrt{2}\epsilon. \quad (150)$$

Similarly, for the state of infinite finite stellar rank $|\psi_2\rangle$ that is close in trace distance to the state of finite stellar rank $|F_2\rangle$:

$$T(|\psi_2\rangle\langle\psi_2|, |F_2\rangle\langle F_2|) \leq \epsilon_2 \implies \left| |\langle F_1|\psi_2\rangle| - |\langle F_1|F_2\rangle| \right| \leq \sqrt{2}\epsilon_2. \quad (151)$$

Eqs. (150) and (151) can be combined to bound on the inner product of two states of infinite stellar rank,

$$\begin{aligned}
|\langle \psi_1 | \psi_2 \rangle| &= |\langle \psi_1 - \tilde{F}_1 + \tilde{F}_1 | \psi_2 \rangle| \\
&= |\langle \psi_1 - \tilde{F}_1 | \psi_2 \rangle + \langle \tilde{F}_1 | \psi_2 \rangle| \\
&\leq |\langle \psi_1 - \tilde{F}_1 | \psi_2 \rangle| + |\langle \tilde{F}_1 | \psi_2 \rangle| \\
&\leq \sqrt{2}\epsilon + |\langle F_1 | \psi_2 \rangle| && \text{(Eqs. (143) \& (144))} \\
&\leq \sqrt{2}\epsilon + |\langle F_1 | F_2 \rangle| + \sqrt{2}\epsilon_2 && \text{(Eq. (151))} \\
&= |\langle F_1 | F_2 \rangle| + \sqrt{2}(\epsilon + \epsilon_2).
\end{aligned} \tag{152}$$

Therefore

$$|\langle \psi_1 | \psi_2 \rangle| - |\langle F_1 | F_2 \rangle| \leq 2\sqrt{2} \tilde{\epsilon} \tag{153}$$

where

$$\tilde{\epsilon} := \max(\epsilon, \epsilon_2). \tag{154}$$

And

$$\begin{aligned}
|\langle F_1 | F_2 \rangle| &\leq |\langle F_1 | \psi_2 \rangle| + \sqrt{2}\epsilon_2 && \text{(Eq. (151))} \\
&= |\langle \tilde{F}_1 | \psi_2 \rangle| + \sqrt{2}\epsilon_2 && \text{(Eq. (143))} \\
&= |\langle \tilde{F}_1 - \psi_1 + \psi_1 | \psi_2 \rangle| + \sqrt{2}\epsilon_2 \\
&= |\langle \tilde{F}_1 - \psi_1 | \psi_2 \rangle + \langle \psi_1 | \psi_2 \rangle| + \sqrt{2}\epsilon_2 \\
&\leq |\langle \tilde{F}_1 - \psi_1 | \psi_2 \rangle| + |\langle \psi_1 | \psi_2 \rangle| + \sqrt{2}\epsilon_2 \\
&\leq \sqrt{2}\epsilon + |\langle \psi_1 | \psi_2 \rangle| + \sqrt{2}\epsilon_2 && \text{(Eq. (144))} \\
&= |\langle \psi_1 | \psi_2 \rangle| + \sqrt{2}(\epsilon + \epsilon_2).
\end{aligned} \tag{155}$$

Therefore

$$|\langle F_1 | F_2 \rangle| - |\langle \psi_1 | \psi_2 \rangle| \leq 2\sqrt{2} \tilde{\epsilon} \tag{156}$$

and combining Eqs. (153) and (156) gives

$$\left| |\langle \psi_1 | \psi_2 \rangle| - |\langle F_1 | F_2 \rangle| \right| \leq 2\sqrt{2} \tilde{\epsilon}. \tag{157}$$

Finally, using the fact that

$$|\langle \psi_1 | \psi_2 \rangle|, |\langle F_1 | F_2 \rangle| \in [0, 1] \implies \left(|\langle \psi_1 | \psi_2 \rangle| + |\langle F_1 | F_2 \rangle| \right) \in [0, 2] \tag{158}$$

it can be shown that

$$\begin{aligned}
|\langle \psi_1 | \psi_2 \rangle|^2 - |\langle F_1 | F_2 \rangle|^2 &= \left(|\langle \psi_1 | \psi_2 \rangle| - |\langle F_1 | F_2 \rangle| \right) \left(|\langle \psi_1 | \psi_2 \rangle| + |\langle F_1 | F_2 \rangle| \right) \\
&\leq 2\sqrt{2} \tilde{\epsilon} \left(|\langle \psi_1 | \psi_2 \rangle| + |\langle F_1 | F_2 \rangle| \right) \\
&\leq 4\sqrt{2} \tilde{\epsilon}
\end{aligned} \tag{159}$$

and

$$\begin{aligned}
|\langle F_1 | F_2 \rangle|^2 - |\langle \psi_1 | \psi_2 \rangle|^2 &= \left(|\langle F_1 | F_2 \rangle| - |\langle \psi_1 | \psi_2 \rangle| \right) \left(|\langle F_1 | F_2 \rangle| + |\langle \psi_1 | \psi_2 \rangle| \right) \\
&\leq 2\sqrt{2} \tilde{\epsilon} \left(|\langle F_1 | F_2 \rangle| + |\langle \psi_1 | \psi_2 \rangle| \right) \\
&\leq 4\sqrt{2} \tilde{\epsilon}
\end{aligned} \tag{160}$$

so

$$\left| |\langle \psi_1 | \psi_2 \rangle|^2 - |\langle F_1 | F_2 \rangle|^2 \right| \leq 4\sqrt{2} \tilde{\epsilon}. \quad (161)$$

In other words the kernel defined by CV states of infinite stellar rank can be approximated arbitrarily well by a CV kernel of finite stellar rank

$$|k_\infty(x, x') - k_n(x, x')| \leq 4\sqrt{2} \tilde{\epsilon} \quad (162)$$

G Calculation of the qudit kernel

In this section we show the details of the calculation of the qudit kernel (Eq.(53)),

In the function representation, the inner product of two qudits is

$$\begin{aligned} \langle F_1^*(z) | F_1^*(z) \rangle &= \frac{1}{\pi} \int_{z \in \mathbb{C}} dz^2 e^{-z^2} \left(\sum_{i=0}^{d-1} n_{d,i}^* \alpha_i^{(1)*} (z^*)^i \right) \left(\sum_{j=0}^{d-1} n_{d,j} \alpha_j^{(2)} z^j \right) \\ &= \frac{1}{\pi} \sum_{i=0}^{d-1} \sum_{j=0}^{d-1} n_{d,i}^* n_{d,j} \alpha_i^{(1)*} \alpha_j^{(2)} \int_{-\infty}^{\infty} dx \int_{-\infty}^{\infty} dy e^{-(x^2+y^2)} (x-iy)^i (x+iy)^j \\ &= \frac{1}{\pi} \sum_{i=0}^{d-1} \sum_{j=0}^{d-1} n_{d,i}^* n_{d,j} \alpha_i^{(1)*} \alpha_j^{(2)} \sum_{p=0}^i \sum_{q=0}^j \binom{i}{p} \binom{j}{q} (-i)^p (i)^q \left(\int_{-\infty}^{\infty} dy e^{-y^2} y^{p+q} \right) \\ &\quad \times \left(\int_{-\infty}^{\infty} dx e^{-x^2} x^{i+j-p-q} \right) \\ &= \frac{1}{\pi} \sum_{i=0}^{d-1} \sum_{j=0}^{d-1} n_{d,i}^* n_{d,j} \alpha_i^{(1)*} \alpha_j^{(2)} \sum_{p=0}^i \sum_{q=0}^j \binom{i}{p} \binom{j}{q} (-i)^p (i)^q \left(\frac{1+(-1)^{p+q}}{2} \Gamma\left(\frac{1+p+q}{2}\right) \right) \\ &\quad \times \left(\frac{1+(-1)^{i+j-p-q}}{2} \Gamma\left(\frac{1+i+j-p-q}{2}\right) \right) \\ &= \frac{1}{\pi} \sum_{i=0}^{d-1} \sum_{j=0}^{d-1} \frac{1+(-1)^{i+j}}{2} n_{d,i}^* n_{d,j} \alpha_i^{(1)*} \alpha_j^{(2)} \sum_{p=0}^i \sum_{q=0}^j (-1)^q \binom{i}{p} \binom{j}{q} \cos\left(\frac{\pi(p+q)}{2}\right) \\ &\quad \times \Gamma\left(\frac{1+p+q}{2}\right) \Gamma\left(\frac{1+i+j-p-q}{2}\right) \end{aligned} \quad (163)$$

where each term the sum is zero unless both $(i+j)$ and $(p+q)$ are even. Now using the fact that

$$\Gamma\left(\frac{1}{2} + n\right) = \sqrt{\pi} \frac{(2n)!}{4^n n!} \quad (164)$$

the qudit inner product becomes

$$\begin{aligned} \langle F_1^*(z) | F_1^*(z) \rangle &= \frac{1}{\pi} \sum_{i=0}^{d-1} \sum_{j=0}^{d-1} \frac{1+(-1)^{i+j}}{2} n_{d,i}^* n_{d,j} \alpha_i^{(1)*} \alpha_j^{(2)} \sum_{p=0}^i \sum_{q=0}^j (-1)^q \binom{i}{p} \binom{j}{q} \cos\left(\frac{\pi(p+q)}{2}\right) \\ &\quad \times \left(\sqrt{\pi} \frac{(p+q)!}{4^{(p+q)/2} (p+q)/2)!} \right) \left(\sqrt{\pi} \frac{(i+j-p-q)!}{4^{(i+j-p-q)/2} (i+j-p-q)/2)!} \right) \\ &= \sum_{i=0}^{d-1} \sum_{j=0}^{d-1} \frac{1+(-1)^{i+j}}{2} \frac{1}{2^{(i+j)}} n_{d,i}^* n_{d,j} \alpha_i^{(1)*} \alpha_j^{(2)} \sum_{p=0}^i \sum_{q=0}^j (-1)^q \binom{i}{p} \binom{j}{q} \cos\left(\frac{\pi(p+q)}{2}\right) \\ &\quad \times \frac{(p+q)!}{(p+q)/2)!} \frac{(i+j-p-q)!}{(i+j-p-q)/2)!}. \end{aligned} \quad (165)$$

G.1 Calculation of the qudit kernel from the general multi-mode kernel

In this section, we calculate the qudit kernel from the general multi-mode kernel (Eq. (46)).

First we note that when $x = 0$

$$\sum_{j=0}^n \alpha_j x^j = \sum_{j=0}^n \alpha_j \delta_{j,0} = \alpha_0. \quad (166)$$

Since a qudit can always be represented as a function of a single complex variable, we set $m = 1$. Additionally from Eq. (50) we find that

$$\begin{aligned} a_{0,j} &= 1 \\ b_{0,j} &= 0 \\ d_{0,j,k} &= 0 \\ C^{(1)} &= C^{(2)} = 0 \end{aligned}$$

and by the recursion relations (Eq. (47))

$$\begin{aligned} a_{i,j} &= 1 \\ b_{i,j} &= 0 \\ d_{i,j,k} &= 0. \end{aligned}$$

Now the inner product becomes

$$\begin{aligned} \langle F_1^\star(z) | F_2^\star(z) \rangle &= \frac{1}{\pi} \sum_{i=0}^n \sum_{j=0}^n \beta_i^{(1)*} \beta_j^{(2)} \sum_{p=0}^i \sum_{q=0}^j \sum_{s_1=0}^{r_{0,1}} \gamma_{r_{0,1},s_1} \sum_{t_1=0}^{s_1} \frac{s_1!}{(s_1 - t_1)!} \delta_{t_1,s_1} g_{1,2} \sum_{s_2=0}^{r_{1,2}} \gamma_{r_{1,2},s_2} \delta_{s_2,0} \\ &= \frac{1}{\pi} \sum_{i=0}^n \sum_{j=0}^n \beta_i^{(1)*} \beta_j^{(2)} \sum_{p=0}^i \sum_{q=0}^j \sum_{s_1=0}^{r_{0,1}} \gamma_{r_{0,1},s_1} \sum_{t_1=0}^{s_1} \frac{s_1!}{(s_1 - t_1)!} \delta_{t_1,s_1} \left(\frac{g_{0,2}}{t_1!} \delta_{t_1,0} \right) \\ &\quad \times \sum_{s_2=0}^{r_{0,2}+t_1} \gamma_{r_{0,2}+t_1,s_2} \delta_{s_2,0} \\ &= \frac{1}{\pi} \sum_{i=0}^n \sum_{j=0}^n \beta_i^{(1)*} \beta_j^{(2)} \sum_{p=0}^i \sum_{q=0}^j \gamma_{r_{0,1},0} g_{0,2} \gamma_{r_{0,2},0} \\ &= \frac{1}{\pi} \sum_{i=0}^n \sum_{j=0}^n \beta_i^{(1)*} \beta_j^{(2)} \sum_{p=0}^i \sum_{q=0}^j \gamma_{p+q,0} \left(\binom{i}{p} \binom{j}{q} (-i)^p (i)^q \right) \gamma_{i+j-p-q,0} \end{aligned} \quad (167)$$

where in the second line, we substitute in the recursion relations for g and r (Eq. (48)) and in the fourth line we substitute in the initial values of g and r (Eq. (126)).

From Eq. (27),

$$\begin{aligned} \gamma_{r,0} &= \begin{cases} \Gamma\left(\frac{1+r}{2}\right), & r \text{ even} \\ 0, & \text{otherwise} \end{cases} \\ &= \frac{1 + (-1)^r}{2} \Gamma\left(\frac{1+r}{2}\right) \end{aligned} \quad (168)$$

and so

$$\begin{aligned}
\langle F_1^\star(z) | F_2^\star(z) \rangle &= \frac{1}{\pi} \sum_{i=0}^n \sum_{j=0}^n \beta_i^{(1)*} \beta_j^{(2)} \sum_{p=0}^i \sum_{q=0}^j \binom{i}{p} \binom{j}{q} (-i)^p (i)^q \\
&\quad \times \left(\frac{1 + (-1)^{p+q}}{2} \Gamma \left(\frac{1+p+q}{2} \right) \right) \left(\frac{1 + (-1)^{i+j-p-q}}{2} \Gamma \left(\frac{1+i+j-p-q}{2} \right) \right)
\end{aligned} \tag{169}$$

which matches the result from directly integrating the qudit inner product (Eq. (163)) for $n = d - 1$ and $\beta_j = \mathbf{n}_{d,j} \alpha_j$.